developmentally regulated manner.[23] Upregulation of these proteins could accelerate chondrocyte hypertrophy and final maturation of hypertrophic chondrocytes. Wnt/β-catenin signaling is also thought to act downstream of Ihh signaling in enchondral ossification.[23] The downstream signal of Ihh suppresses Wnt/β-catenin signaling and prevents proliferating chondrocytes from final maturation and differentiation. Although the interaction of Ihh signaling and Wnt/β-catenin signaling in OPLL remains unclear, we suggested that Ihh signaling induces chondrocyte hypertrophy whereas suppresses Wnt/β-catenin signaling in the early stage of OPLL progression. Furthermore, Ihh signaling may release the suppression of Wnt/β-catenin signaling in the late stage, and finally, differentiation of mature chondrocytes is accelerated by upregulation of the Wnt/β-catenin signaling. This scenario may play an important role in the progression of OPLL.

In conclusion, our results demonstrated the expression of Ihh in the ossification front in OPLL and that its expression level was higher in cells derived from OPLL. The results suggest that Ihh signaling may be an important factor in OPLL, and the expression of PTHrP and Sox9, which are involved in Ihh signaling, may contribute to the maturation and differentiation of chondrocytes during progression in OPLL. The present study was limited to the examination of factors involved in only one aspect of chondrocyte differentiation. Further studies are needed both to examine chondrocyte and osteoblast differentiation and to determine whether the accumulation of mesenchymal cells initiates the ossification process. If we could regulate cell differentiation by controlling the cell signaling pathway, we might be able to maintain the homeostatic balance of chondrocyte/osteocyte differentiation and prevent the ossification of spinal ligaments.

➢ Key Points

- ❑ OPLL specimens showed enchondral ossification with the presence of chondrocytes at various stages of differentiations.
- ❑ Hypertrophic chondrocytes were present in calcified cartilaginous area, and apoptotic chondrocytes appeared near the ossified area.
- ❑ Proliferating chondrocytes were positive for Ihh, PTHrP, and Sox9, whereas hypertrophic chondrocytes were strongly positive for PTHrP.
- ❑ Cultured cells derived from OPLL samples expressed high levels of Ihh, PTHrP, and Sox9 compared with non-OPLL samples.

Acknowledgments

We thank Dr. Hitoshi Takagi, Life Science Research Laboratory, Division of Bioresearch, Fukui University, for the excellent technical assistance.

None of authors has any financial interest in any of the commercial entities mentioned in this article.

Supplemental digital content is available for this article. Direct URL citations appear in the printed text and are provided in the HTML and PDF versions of this article on the journal's Web site (www.spinejournal.com).

References

1. White AA III, Panjabi MM. Physical properties and functional biomechanics of the spine. In: White AA III, Panjabi MM, eds. *Clinical Biomechanics of the Spine*. 2nd ed. Philadelphia: Lippincott-Raven; 1990:19–28.
2. Hayashi K, Yabuki T, Kurokawa T, et al. The anterior and the posterior longitudinal ligaments of the lower cervical spine. *J Anat* 1977;124:633–6.
3. Okamoto K, Kobayashi G, Washio M, et al. Dietary habits and risk of ossification of the posterior longitudinal ligaments of the spine (OPLL): findings from a case-control study in Japan. *J Bone Miner Metab* 2004;22:612–7.
4. Ramos-Remus C, Russel AS, Gomez-Vargas A, et al. Ossification of the posterior longitudinal ligament in three geographically and genetically different populations of ankylosing spondylitis and other spondyloarthropathies. *Ann Rheum Dis* 1998;57:429–33.
5. Shingyouchi Y, Nagahama A, Niida M. Ligamentous ossification of the cervical spine in the late middle-aged Japanese men. Its relation to body mass index and glucose metabolism. *Spine* 1996;21: 2474–8.
6. Matsunaga S, Sakou T. OPLL: disease entity, incidence, literature search, and prognosis. In: Yonenobu K, Nakamura K, Toyama Y, eds. *OPLL*. 2nd ed. Tokyo: Springer; 2006:11–7.
7. Furushima K, Shimo-Onoda K, Maeda S, et al. Large-scale screening for candidate genes of ossification of the posterior longitudinal ligament of the spine. *J Bone Miner Res* 2002;17:128–37.
8. Horikoshi T, Maeda K, Kawaguchi Y, et al. A large-scale genetic association study of ossification of the posterior longitudinal ligament of the spine. *Hum Genet* 2006;119:611–6.
9. Karasugi T, Nakajima M, Ikari K, et al. A genome-wide sib-pair linkage analysis of ossification of the posterior longitudinal ligament of the spine. *J Bone Miner Metab* 2013;31:136–43.
10. Hashizume Y. Pathological studies on the ossification of the posterior longitudinal ligament (OPLL). *Acta Pathol Jpn* 1980;30: 255–73.
11. Liao CC, Lee ST. Symptomatic ossification of the posterior longitudinal ligament of the lumbar spine. Case report. *J Neurosurg* 1999;91:230–2.
12. Baba H, Furusawa N, Tomita K, et al. Potential role of streptozotocin in enhancing ossification of the posterior longitudinal ligament of the cervical spine in the hereditary spinal hyperostotic mouse (*twy/twy*). *Eur J Histochem* 1997;41:191–202.
13. Sato R, Uchida K, Baba H, et al. Ossification of the posterior longitudinal ligament of the cervical spine: histopathological findings around the calcification and ossification front. *J Neurosurg Spine* 2007;7:174–83.
14. Yayama T, Uchida K, Baba H, et al. Thoracic ossification of the human ligamentum flavum: histopathological and immunohistochemical findings around the ossified lesion. *J Neurosurg Spine* 2007;7:184–93.
15. Uchida K, Yayama T, Baba H, et al. Ossification process involving the human thoracic ligamentum flavum: role of transcriptional factors. *Arthritis Res Ther* 2011;13:R144.
16. Cai HX, Yayama T, Baba H, et al. Cyclic tensile strain facilitates the ossification of ligamentum flavum through β-catenin signaling pathway. *In vitro* analysis. *Spine* 2011;37:639–46.
17. Kawaguchi H, Kurokawa T, Hoshino Y, et al. Immunohistochemical demonstration of bone morphogenetic protein-2 and transforming growth factor-beta in the ossification of the posterior longitudinal ligament of the cervical spine. *Spine* 1992;17:33–6.
18. Tsukamoto N, Maeda T, Miura H, et al. Repetitive tensile strain stress to rat caudal vertebrae inducing cartilage formation in the spinal ligaments: a possible role of mechanical stress in the development of the ossification of the spinal ligaments. *J Neurosurg Spine* 2006;5:234–42.

19. St-Jacques B, Hammerschmidt M, McMahon AP. Indian hedgehog signaling regulates proliferation and differentiation of chondrocytes and is essential for bone formation. *Genes Dev* 1999;13:2072–86.
20. Lanske B, Karaplis AC, Kronenberg HM, et al. PTH/PTHrP receptor in early development and Indian hedgehog regulated bone growth. *Science* 1996;273:663–6.
21. Stoeger T, Proetzel GE, Hofmann C, et al. *In situ* gene expression analysis during BMP2-induced ectopic bone formation in mice shows simultaneous endochondral and intramembranous ossification. *Growth Factors* 2002;20:197–210.
22. Uchida K, Nakajima H, Baba H, et al. Apoptosis of neurons and oligodendrocytes in the spinal cord in the spinal hyperostotic mouse (*twy/twy*): possible pathomechanism of human cervical compressive myelopathy. *Eur Spine J* 2012;21:490–7.
23. Day TF, Yang Y. Wnt and hedgehog signaling pathways in bone development. *J Bone Joint Surg Am* 2008;90:19–24.
24. Yang Y, Topol L, Lee H, et al. Wnt5a and Wnt5b exhibit distinct activities in coordinating chondrocytes proliferation and differentiation. *Development* 2003;130:1003–15.
25. Izzo MW, Pucci B, Tuan RS, et al. Gene expression profiling following BMP-2 induction of mesenchymal chondrogenesis *in vitro*. *Osteoarthritis Cartilage* 2002;10:23–33.
26. Scmid TM, Linsenmayer TF. Immunoelectron microscopy of type X collagen: supramolecular forms within embryonic chick cartilage. *Dev Biol* 1990;138:53–62.
27. Li Y, Lacerda DA, Warman ML, et al. A fibrillar collagen gene, *Col11a1*, is essential for skeletal morphogenesis. *Cell* 1995;80:423–30.
28. Anderson HC. Molecular biology of matrix vesicles. *Clin Orthop Relat Res* 1995;314:266–80.
29. Zelzer E, Glotzer DJ, Hartmann C, et al. Tissue specific regulation of VEGF expression during bone development requires Cbfa1/Runx2. *Mech Dev* 2001;106:97–106.
30. Kronenberg HM. Developmental regulation of the growth plate. *Nature* 2003;423:332–6.
31. Ikeda T, Kawaguchi H, Kamekura S, et al. Distinct roles of Sox5, Sox6 and Sox0 in different stages of chondrogenic differentiation. *J Bone Miner Metab* 2005;23:337–40.
32. Komori T. Regulation of osteoblast differentiation by transcriptional factors. *J Cell Biochem* 2006;99:1233–9.
33. Ehlen H, Buelens LA, Vortkamp A. Hedgehog signaling in skeletal development. *Birth Defects Res C Embryo Today* 2006;78:267–79.
34. Koyama E, Leatherman JL, Noji S, et al. Early chick limb cartilaginous elements possess polarizing activity and express hedgehog-related morphogenetic factors. *Dev Dyn* 1996;207:344–54.
35. Nakamura T, Aikawa T, Iwamoto-Enomoto M, et al. Induction of osteogenic differentiation by hedgehog proteins. *Biochem Biophys Res Commun* 1997;237:4655–69.
36. Vortkamp A, Lee K, Lanske B, et al. Parathyroid hormone-related peptide delays terminal differentiation of chondrocytes during endochondral bone development. *Endocrinology* 1996;137:5109–18.
37. Mak KK, Kronenberg HM, Chuang PT, et al. Indian hedgehog signals independently of PTHrP to promote chondrocyte hypertrophy. *Development* 2008;135:1947–56.
38. Shimoyama A, Wada M, Yoneda T, et al. Ihh/Gli2 signaling promotes osteoblast differentiation by regulating Runx2 expression and function. *Mol Biol Cell* 2007;18:2411–8.
39. Amano K, Hata K, Yoneda T, et al. Sox9 family members negatively regulate maturation and calcification of chondrocytes through up-regulation of parathyroid hormone-related protein. *Mol Biol Cell* 2009;20:4541–51.
40. Song J, Mizuno J, Hashizume Y, et al. Immunohistochemistry of symptomatic hypertrophy of the posterior longitudinal ligament with special reference to ligamentous ossification. *Spinal Cord* 2006;44:576–81.

J Neuropathol Exp Neurol

Vol. 72, No. 10
October 2013
pp. 980–993

ORIGINAL ARTICLE

Blockade of Interleukin 6 Signaling Improves the Survival Rate of Transplanted Bone Marrow Stromal Cells and Increases Locomotor Function in Mice With Spinal Cord Injury

Ying Tan, MD, Kenzo Uchida, MD, PhD, Hideaki Nakajima, MD, PhD, Alexander R. Guerrero, MD, Shuji Watanabe, MD, Takayuki Hirai, MD, Naoto Takeura, MD, Shao-Yu Liu, MD, PhD, William E.B. Johnson, PhD, and Hisatoshi Baba, MD, PhD

Abstract

Bone marrow stromal cells (BMSCs) have the potential to improve functional recovery in patients with spinal cord injury (SCI); however, they are limited by low survival rates after transplantation in the injured tissue. Our objective was to clarify the effects of a temporal blockade of interleukin 6 (IL-6)/IL-6 receptor (IL-6R) engagement using an anti-mouse IL-6R monoclonal antibody (MR16-1) on the survival rate of BMSCs after their transplantation in a mouse model of contusion SCI. MR16-1 cotreatment improved the survival rate of transplanted BMSCs, allowing some BMSCs to differentiate into neurons and astrocytes, and improved locomotor function recovery compared with BMSC transplantation or MR16-1 treatment alone. The death of transplanted BMSCs could be mainly related to apoptosis rather than necrosis. Transplantation of BMSC with cotreatment of MR16-1 was associated with a decrease of some proinflammatory cytokines, an increase of neurotrophic factors, decreased apoptosis rates of transplanted BMSCs, and enhanced expression of survival factors Akt and extracellular signal–regulated protein kinases 1/2. We conclude that MR16-1 treatment combined with BMSC transplants helped rescue neuronal cells and axons after contusion SCI better than BMSCs alone by modulating the inflammatory/immune responses and decreasing apoptosis.

Key Words: Apoptosis, Bone marrow stromal cells, Cell survival, Inflammation, Interleukin 6, Spinal cord injury, Transplantation.

From the Department of Spine Surgery, The First Affiliated Hospital, Sun Yat-Sen University, Guangzhou, People's Republic of China (YT, SYL); Department of Orthopaedics and Rehabilitation Medicine, Faculty of Medical Sciences, University of Fukui, Fukui, Japan (YT, KU, HN, ARG, SW, TH, NT, HB); and Life and Health Sciences, Aston University, Aston Triangle, Birmingham, United Kingdom (WEBJ).

Send correspondence and reprint requests to: Kenzo Uchida, MD, PhD, Department of Orthopaedics and Rehabilitation Medicine, Faculty of Medical Sciences, University of Fukui, Matsuoka Shimoaizuki 23-3, Eiheiji, Fukui 910-1193, Japan; E-mail: kuchida@u-fukui.ac.jp

This work was supported in part by grants-in-aid to Hisatoshi Baba and Kenzo Uchida for General Scientific Research of the Ministry of Education, Science and Culture of Japan (No. B-22390287 and No. B-24390351).

The authors do not have a financial interest or other relationship with any commercial company or institution.

Supplemental digital content is available for this article. Direct URL citations appear in the printed text and are provided in the HTML and PDF versions of this article on the journal's Web site (www.jneuropath.com).

INTRODUCTION

Spinal cord injury (SCI) is a complex and variable process that develops in distinct temporal stages; often, there is an expansion of the initially damaged area and persistent loss of function. The lack of recovery after SCI is thought to result from a failure of axonal regeneration that has been attributed to the development of a nonpermissive microenvironment within the injured tissue in which there are inflammatory mediators that increase neuroglial cell death, a lack of neurotrophic support, and the formation of cysts and a glial scar (1–5). Therefore, aggressive treatments that may reconstruct permissive microenvironments for neuronal regeneration would be beneficial; these could both prevent neuronal tissue loss and cyst and glial scar formation after the injury, as well as promote axonal growth and regeneration.

A variety of experimental strategies including stem cell transplantation are emerging to promote regeneration of the injured spinal cord and recovery of function. The injection of bone marrow–derived mesenchymal stromal or stem cells (bone marrow stromal cells [BMSCs]) into the injured spinal cord may provide clinical advantages over other stem cell types (6–8). Bone marrow stromal cells can be readily harvested, expanded, and stored from donors but also obtained directly from the patient (9), allowing for autologous transplantation and thereby avoiding immunologic and potential ethical or safety issues linked to embryonic and induced pluripotent stem cells. One major mechanism by which BMSCs may promote functional recovery after SCI is through their secretion of a broad spectrum of bioactive macromolecules that are trophic or immunoregulatory and that could contribute to the restructuring of the nonpermissive wound microenvironment. In particular, we have shown that BMSC transplantation after acute SCI is associated with a reduction in the presence of inflammatory mediators (10). Other possible mechanisms include the potential for BMSCs to remyelinate axons directly (11), to transdifferentiate to form neurons (12), and to provide a bridging effect for axonal regeneration across the injury site (13). All of these mechanisms have been demonstrated in vivo; however, the application of BMSCs is limited by their poor survival when transplanted into the injured spinal cord (14–16). In fact, some studies have suggested that the survival rate of transplanted BMSCs correlates with improvement of tissue

repair (14). One likely major cause for the loss of BMSCs is the inflammation that occurs in the injury site as a result of the SCI or the immediate inflammatory response elicited by the cell transplantation procedure (17, 18). Therefore, combination therapy that provides support to transplanted cells by suppressing acute inflammation may increase the survival of grafted cells as well as benefiting behavioral outcomes.

The primary mechanical injury in SCI is followed by posttraumatic inflammation in which inflammatory cells such as neutrophils, hematogenous macrophages, and resident microglia accumulate at the lesion site. These inflammatory cells release reactive oxygen radicals and proteases that exacerbate tissue damage (3). Because the inflammation is regulated by proinflammatory cytokines, such as tumor necrosis factor (TNF), interleukin 1β (IL-1β), and IL-6; these cytokines have been targeted for potential pharmaceutical interventions for SCI (19, 20). Among these, IL-6 is an early and key factor that triggers the inflammatory response after SCI (21–23). Interleukin 6 can enhance the expression of other inflammatory cytokines, including TNF and IL-1β (21, 24). Complete blockade of IL-6 has detrimental effects on recovery from SCI, perhaps reflecting the requirement of inflammation for spinal cord regeneration (25). Indeed, a transient blockade of IL-6 has been shown to downregulate the expression of other proinflammatory cytokines in the acute phase of SCI while preserving the beneficial effects of inflammation in the following stages of recovery (26–28).

Based on these previous findings, we hypothesized that temporal blockade of IL-6 may modify the acute-phase inflammatory response after SCI to create permissive microenvironments for neuronal regeneration at the site of injury, which may also improve the low survival of transplanted BMSCs. In the present study, we investigated the effects of temporal blockade of IL-6/IL-6 receptor (IL-6R) engagement during this response using a rat anti-mouse IL-6R monoclonal antibody (i.e. MR16-1) (29). We focused on the potential effects of IL-6 blockade in preventing transplanted cell death, examined the fate of any surviving cells, and determined whether the combination of IL-6 blockade with the transplantation of BMSCs had greater efficacy on functional outcomes than BMSCs or MR16-1 alone.

MATERIALS AND METHODS

Isolation and Enrichment of BMSCs

Bone marrow stromal cells were isolated according to the method described by Soleimani and Nadri (30), with some modifications. In brief, femurs and tibias from transgenic mice that express green fluorescent protein (GFP) driven by the cytomegalovirus early enhancer β-actin (CAG) (so-called CAG-EGFP mice; SLC, Shizuoka, Japan) were removed, and all muscle and extraosseal tissues were removed. Bone marrow cells were flushed, collected, and cultured with Dulbecco modified Eagle medium (Invitrogen Life Technologies, Carlsbad, CA) supplemented with 15% fetal bovine serum and penicillin (100 U/mL)/streptomycin (100 U/mL) (Invitrogen Life Technologies) at 37°C in humid air with 5% CO_2. After 48 hours, the suspended nonadherent cells were removed. The culture medium was changed every 3 days, allowing the cells to grow until almost confluent. Adherent cells were then detached by 0.25% trypsin–EDTA (Invitroge006E) and replaced using 1:3 dilutions until passage 2. Bone marrow stromal cells were used for transplantation experiments between 3 and 4 passages.

Animal Model of SCI

The Ethics Review Committee for Animal Experimentation of the University of Fukui approved the experimental protocol. Experiments were conducted in a total of 162 adult male C57BL/6 mice (Clea, Tokyo, Japan), aged 8 to 10 weeks with a mean body weight of 28.2 ± 0.71 g (±SD). The mice were anesthetized with isoflurane (Forane; Abbott, Tokyo, Japan) administered through a Forane vaporizer (Forawick; Muraco Medical Co., Ltd., Tokyo, Japan), and a complete laminectomy was performed on the 10th thoracic spinal cord level using a surgical microscope (VANOX-S; Olympus Optical, Tokyo, Japan) after exposing the dorsal aspect of the dura mater and taking utmost care to avoid producing any dural tear. A contusion SCI was produced using the Infinite Horizons Impactor (Precision Systems and Instrumentation LLC, Fairfax, VA) with an impact force of 60 kilodynes, as previously described (28, 31). Immediately after injury, the subjects in the cotreatment group (BMSCs + MR16-1; n = 48) received a single intraperitoneal dose (50 μg/g body weight) of MR16-1 antibody (Chugai, Tokyo, Japan), MR16-1 was also administered singly (n = 36), whereas the control group of BMSC transplantation alone (n = 99) received a single dose of saline in the same volume. After surgery, the mice were maintained in an isothermic cage until recovery and housed under a 12-hour light-dark cycle in a bacteria-free biologically clean room with access to food and water ad libitum. They received manual bladder expression twice daily until sphincter control recovered.

GFP-Positive BMSC Transplantation

The relationship between the survival rates of transplanted BMSCs with the time after SCI that the BMSCs were transplanted was initially assessed. Hence, survival of BMSCs was examined at 15 minutes and 1, 3, 7, 14, and 28 days after their transplantation, with the BMSC injections made at 1, 3, 7, and 14 days after injury. In all cases, 1×10^5 BMSCs in 3 μL of culture medium were injected into the contusion epicenter of the SCI using a microsyringe (VANOX-S). To assess BMSC survival, we examined midsagittal sections prepared and randomly selected from the injured portion of the spinal cord that had been harvested from 3 mice per group, that is, where 3 mice per time point of BMSC transplantation and 3 mice per time posttransplantation were analyzed. To count the surviving cells, 3 midsagittal sections were randomly selected. From the epicenter area (0–1 mm caudal and rostral to the epicenter), 20 nonoverlapping high-power fields were chosen for analysis at 400× magnification and the surviving GFP-positive cells were counted by a color image analyzer (MacSCOPE). Having established the number of surviving BMSCs, we used the same technique to transplant 1×10^5 BMSCs 3 days after SCI in the MR16-1–treated group and the non–M16-1–treated control

group for further detailed analysis of the combined effects of BMSC transplant and IL-6 blockade.

Assessment of Locomotor Behavior

Hindlimb motor function was evaluated using the Basso Mouse Scale open-field locomotor test in which the scores range from 0 (no ankle movement) to 9 points (complete functional recovery) (32). Basso Mouse Scale scores were recorded at 28 days after transplantation by 2 independent examiners (Hideaki Nakajima, Shuji Watanabe) blinded to the experimental conditions (n = 6 in each time point). We assessed hindlimb motion mainly to evaluate coordinated movement and stepping. When differences in the Basso Mouse Scale scores between the right and left hindlimbs were detected, we took the average of the 2 scores.

Immunoblot Analysis

Immediately after terminal anesthesia, the damaged spinal cord around the epicenter of the lesion (5 mm in total length) was carefully dissected at 1, 7, and 14 days after transplantation en bloc from the thoracic spine and stored immediately at −80°C in liquid N_2 (n = 3 in each time point). Segments were centrifuged at 15,000 × *g* for 30 seconds using a BioMasher Rapid Homogenization Kit (Funakoshi, Tokyo, Japan) and then solubilized in RIPA lysis buffer 1× (Santa Cruz Biotechnology, Santa Cruz, CA), homogenized, and stored at −80°C. Sodium dodecyl sulfate polyacrylamide gel electrophoresis and Western blotting were performed to determine levels of the cytokines IL-6, TNF, brain-derived neurotrophic factor (BDNF), nerve growth factor (NGF), vascular endothelial growth factor (VEGF), and insulin-like growth factor 1 (IGF-1) using methods previously described (10, 20, 28); each lane was loaded for equal amounts of extracted protein (20 μg per lane).

Immunoreactivity was revealed using a commercially available kit (ECL Advance Western Blot Detection kit; GE Healthcare, Buckinghamshire, UK); the levels of each protein detected were normalized to β-actin.

Flow Cytometry Analysis

Bone marrow stromal cells alone (n = 6) and MR16-1 + BMSC–treated (n = 6) mice were killed at 7 days after transplantation; the damaged spinal cord around the epicenter of the lesion (6 mm in total length) was surgically harvested and digested with 175 U/mL collagenase (Sigma-Aldrich, St. Louis, MO) for 1 hour at 37°C. Extracted cells were washed in Dulbecco modified Eagle medium (Invitrogen Life Technologies) containing 10% fetal bovine serum and filtered to obtain a single-cell suspension, as previously described (28, 33). From this point on, cell counts were performed before every staining step in every sample to maintain a cell density of 1.0×10^6 cells/100 μL. Cells were incubated for 1 hour on ice. For intracellular staining, the cells were resuspended in commercial fixation buffer and treated with permeabilization buffer (both Santa Cruz Biotechnology) followed by resuspension in ice-cold 0.1 mol/L PBS and incubation for 1 hour with rabbit anti-Akt and/or anti–extracellular signal–regulated protein kinase 1/2 (ERK1/2) (both diluted at 1:200) conjugated to peridinin chlorophyll protein (PerCP-Cy5.5; Santa Cruz Biotechnology) (34). The mechanism of transplanted BMSC death (i.e. whether apoptosis or necrosis) was assayed using Annexin V–Percific Blue/propidium iodide (PI) staining (BioLegend, San Diego, CA), where 5 μL of Pacific Blue Annexin V and 10 μL of PI solution were incubated with 100 μL of cell suspension for 15 minutes at 25°C in the dark, then with 400 μL of Annexin V Binding Buffer before flow cytometry (FACS Canto II; Becton Dickinson Biosciences, San Jose, CA). In each test, a minimum of 250,000 cells was analyzed, and the data were processed using BD FACSDiva software (Becton Dickinson Biosciences).

Immunohistochemistry and Terminal Deoxynucleotidyl Transferase–Mediated dUTP-Biotin Nick End Labeling

After deep anesthesia, transcardial perfusion was performed in each mouse, followed by fixation with 4% paraformaldehyde in 0.1 mol/L PBS and postfixed in 10% sucrose in 0.1 mol/L PBS (for 24 hours) and 20% sucrose in 0.1 mol/L PBS (for 24 hours). Serial sagittal frozen sections, 20 μm thick, were cut and mounted from the harvested spinal cord (T helper 8 [Th8] to Th12) on glass slides, fixed with 4% paraformaldehyde in 0.1 mol/L PBS for 5 minutes, and rinsed in PBS.

For immunofluorescence staining, frozen sections were permeabilized with 0.1 mol/L Tris-HCl buffer (pH 7.6) containing 0.3% Triton X-100. The following primary antibodies were diluted in commercial diluent (Antibody Diluent with Background Reducing Components; Dako Cytomation, Carpinteria, CA) and applied at 4°C overnight: anti–neuronal nuclei (NeuN) monoclonal antibody (1:400, mouse IgG; Chemicon International, Temecula, CA) for neurons, anti–glial fibrillary acidic protein (GFAP) monoclonal antibody (1:500, rabbit IgG; Abcam, Cambridge, UK) for astrocytes, anti-reactive immunology protein (RIP) monoclonal antibody (1:400, rabbit IgG; Abcam) as a mature oligodendrocyte-specific marker, anti-microglia/macrophage monoclonal antibody (OX42, 1:100, mouse IgG; Abcam) for microglia/macrophage, anti–caspase-3 polyclonal antibody (caspase-3, 1:200, rabbit IgG; Santa Cruz Biotechnology), anti–caspase-8 polyclonal antibody (caspase-8, 1:200, rabbit IgG; Santa Cruz Biotechnology), anti–caspase-9 polyclonal antibody (caspase-9, 1:200, rabbit IgG; Santa Cruz Biotechnology), anti-pAkt polyclonal antibody (pAkt, 1:100, rabbit IgG; Santa Cruz Biotechnology), or anti-pERK1/2 polyclonal antibody (1:100, goat IgG; Santa Cruz Biotechnology). The secondary antibodies were goat anti-rabbit Alexa-Fluor 568–conjugated antibody or goat anti-mouse Alexa-Fluor 568–conjugated antibody (1:250; Molecular Probes, Eugene, OR).

DNA fragmentation was detected by terminal deoxynucleotidyl transferase–mediated dUTP-biotin nick end labeling (TUNEL) using ApopTag Plus Fluorescein In situ Apoptosis Detection kit (Chemicon International), exactly as described (20).

All images were obtained using a fluorescence microscope (Olympus AX80; Olympus Optical) or a confocal laser-scanning microscope (model TCS SP2; Leica Instruments, Nussloch, Germany). Some sections were counterstained with the nuclear marker DAPI (Abbott Molecular, Des Plaines, IL). To count the merged cells, 3 midsagittal sections were randomly

selected. From the epicenter area (0–1 mm caudal and rostral to the epicenter), 20 nonoverlapping high-power fields were chosen for analysis at 400× magnification and the merged cells were counted using a color image analyzer (MacSCOPE).

Electron Microscopy

Electron microscopy was performed on mice that had BMSC transplants at 3 days after SCI with (or without as a control) an immediate MR16-1 injection (n = 3 mice in each group). Mice were harvested at 7 days after transplantation. After anesthesia, each mouse was fixed with 2.5% glutaraldehyde and 2.5% paraformaldehyde, followed by late fixation in 1% osmium tetroxide for 2 hours. Fixed specimens were dehydrated in a graded series of alcohols, embedded in epoxy resin, and polymerized at 60°C for 2 days. Ultrathin sections were cut with an ultramicrotome, stained with uranyl acetate and lead citrate, and examined with a Hitachi H-7650 transmission electron microscope (Hitachi, Tokyo, Japan).

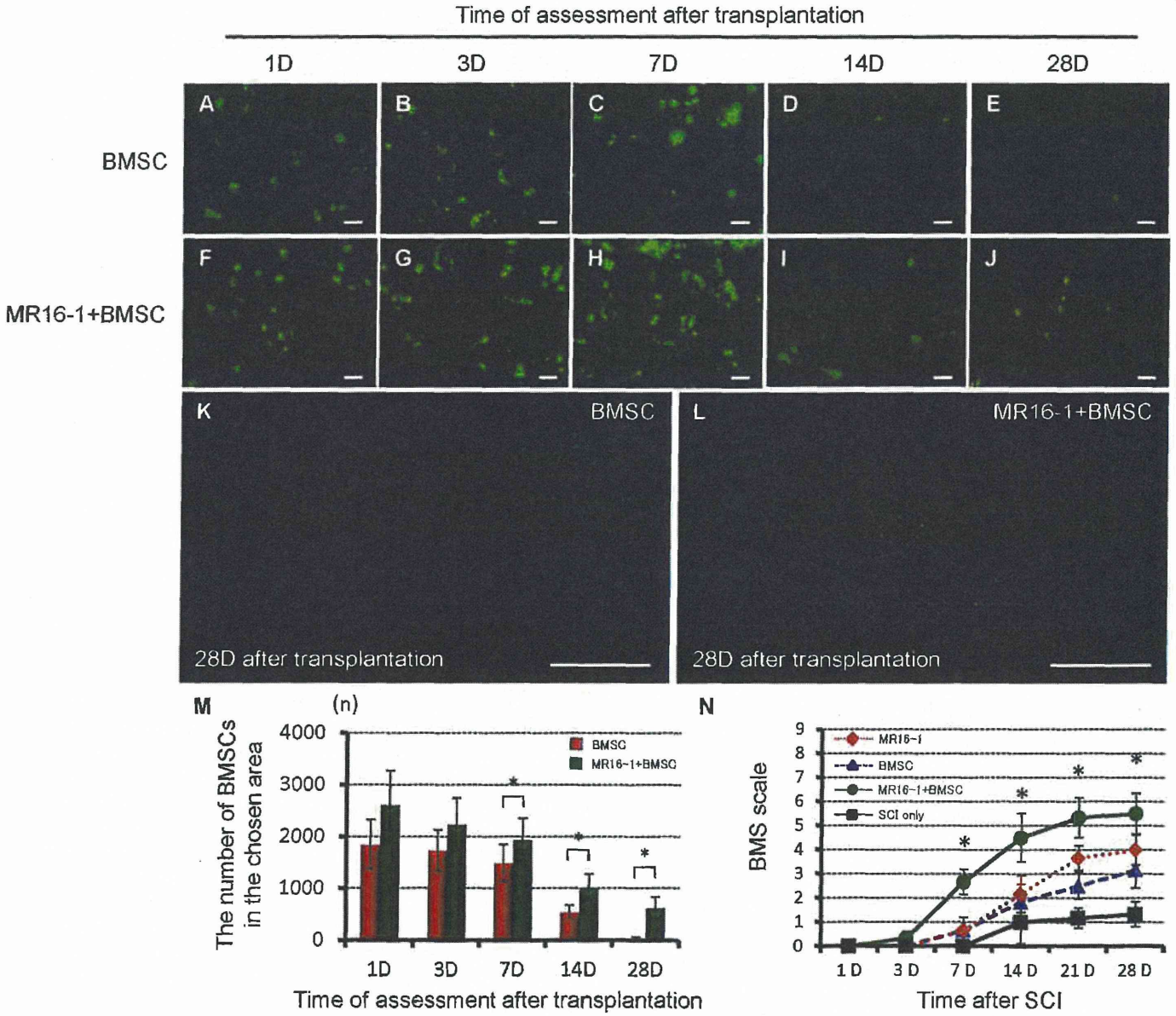

FIGURE 1. Histologic evaluation of the effect of MR16-1 cotreatment on the survival of transplanted bone marrow stromal cells (BMCSs) in spinal cord injury (SCI) and its functional outcome. **(A–L)** BMSCs marked by green fluorescent protein (GFP) and transplanted into 3-day-old injured spinal cords are shown with time after transplantation. The MR16-1 + BMSC cotreatment group **(F–J, L)** versus controls (BMSCs alone) **(A–E, K)** showed significantly increased numbers of surviving transplanted BMSCs from 7 days after transplantation, particularly at 14 and 28 days after transplantation **(M)**. **(N)** Serial changes in locomotor Basso Mouse Scale (BMS) score after SCI. There was a significant improvement in hindlimb motor function in the MR16-1 cotreatment group with transplanted of BMSCs versus the BMSCs alone, MR16-1 alone, and nontreatment (SCI only) groups from 7 days and thereafter after injury. Scale bars = **(A–J)** 25 μm; **(K, L)** 500 μm. * $p < 0.05$.

Statistical Analysis

All values are expressed as mean ± SD. The nonparametric Mann-Whitney U test was used to analyze differences between 2 groups. Kruskal-Wallis test and Games-Howell post hoc test were used to analyze differences among 3 or 4 groups. A value of $p < 0.05$ denotes the presence of a significant difference. The above tests were conducted using SPSS software version 13.0 (SPSS Inc., Chicago, IL).

RESULTS

Characteristics of Isolated BMSCs

Flow cytometric analysis showed that the culture-expanded cells were positive for CD44, CD90, and CD29 (cell surface markers specific for stromal cells) but negative for CD45 and CD11b (markers associated with hematopoietic cells); this is the phenotype of BMSCs (Figure, Supplemental Digital Content 1, http://links.lww.com/NEN/A502).

Relationship Between Survival Rate of Transplanted BMSCs and Time of Transplantation

To determine the appropriate time of BMSC transplantation before the examination of the effect of MR16-1 treatment, the relationship between survival rate of transplanted BMSCs and time of transplantation after injury was examined. In all cases (i.e. at all times after SCI of BMSC transplants), there was a decrease in the presence of GFP-positive cells with time. By 28 days after BMSC transplants, very few or no viable BMSCs were observed; however, the number of surviving BMSCs that had been transplanted at 1 or 3 days after SCI was markedly greater than the number of surviving BMSCs that were transplanted at 7 or 14 days after SCI, with the greatest surviving number seen when BMSCs were transplanted at 3 days after SCI (Figure, Supplemental Digital Content 2, http://links.lww.com/NEN/A503). Based on these results, we determined that the optimal time to examine the effects of MR16-1 cotreatment with BMSC transplantation

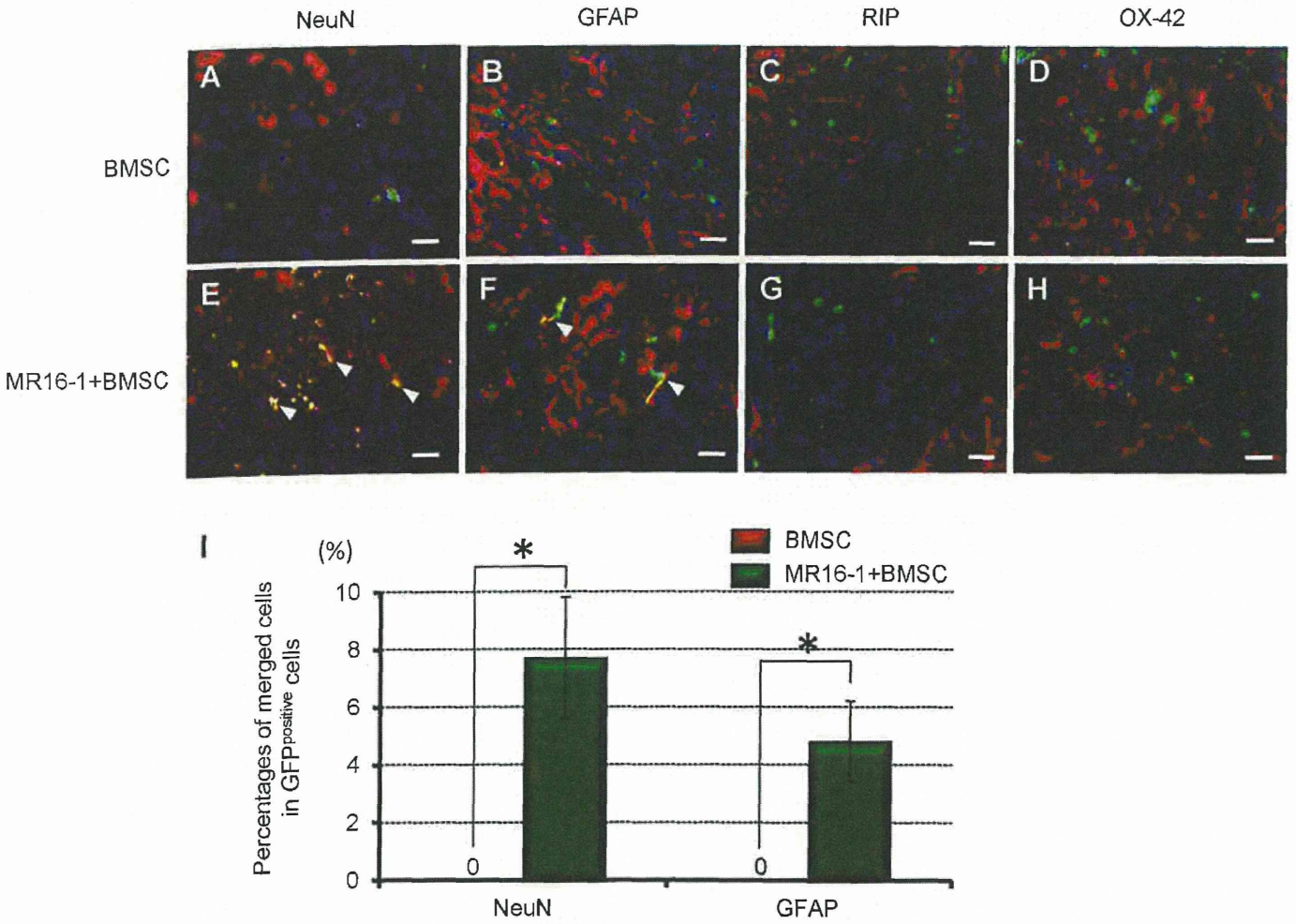

FIGURE 2. Colocalization of neuronal nuclei (NeuN), glial fibrillary acidic protein (GFAP), reactive immunology protein (RIP), OX-42, and green fluorescent protein (GFP)–positive bone marrow stromal cells (BMSCs) in the injured spinal cord at 14 days after spinal cord injury. **(A–H)** BMSCs did not express markers for neurons, astrocytes, oligodendrocytes, or microglia/macrophages in the control group (BMSCs alone), whereas there were GFP-positive BMSCs colocalized with NeuN and GFAP in the MR16-1 + BMSC cotreatment group (white arrowheads). **(I)** Graph shows the percentages of colocalized GFP-positive cells with NeuN- and GFAP-positive cells in the control and MR16-1 + BMSC cotreatment groups. Scale bars = **(A, E)** 50 μm; **(B–D, F–H)** 25 μm. * $p < 0.05$.

was when BMSCs were transplanted at 3 days after SCI because any enhancement of cell survival seen after this time point might be less likely to occur. Henceforth, the results shown evaluating the effects of MR16-1 cotreatment are in mice that were transplanted with BMSCs at 3 days after SCI.

MR16-1 Cotreatment Increases the Survival Rate of Transplanted BMSCs and Improves Locomotor Function After SCI

In the 3 days delayed BMSC transplantation group, the number of GFP-positive BMSCs within the contusion area was significantly larger in the MR16-1 cotreatment group than the control group (BMSCs alone) at 7, 14, and 28 days after transplantation (Fig. 1). The survival rate at 28 days after transplantation was markedly different between the 2 groups (17.8% vs 1.2%) as shown in the sagittal sections (Fig. 1K, L).

Significant motor disturbance in the hindlimbs was noted in mice of the BMSC alone group (SCI + BMSCs) and MR16-1 alone group (SCI + MR16-1), although some degree of recovery was evident subsequently, which reached a functional plateau at 28 days after SCI. In contrast, the cotreatment group of MR16-1 + BMSC transplants (SCI + MR16-1 + BMSCs) showed a significantly increased Basso Mouse Scale score compared with both of these single-treatment groups (BMSCs alone or MR16-1 alone) from 7 days after SCI and thereafter (Fig. 1N).

BMSCs in MR16-1–Treated Mice Transdifferentiated Toward Neuronal Lineages

To investigate the differentiation status of surviving BMSCs, immunostaining of spinal cord sections for NeuN, RIP, GFAP, and OX-42 was performed at 14 days after transplantation of BMSCs in the 3 days delayed transplantation group. In the control group (BMSCs alone), there was no obvious colocalization of NeuN, GFAP, RIP, or OX-42 with GFP-identified BMSCs. However, in the MR16-1 cotreatment group, there were GFP-positive cells colocalized with NeuN (7.7% ± 2.1%; 79.7 ± 21.7 cells) and GFAP (4.8% ± 1.4%; 49.7 ± 14.5 cells) (Fig. 2); no colocalization with RIP and OX-42 was found. These results indicated that some BMSCs may have the potential to transdifferentiate into neurons and astrocytes under conditions that promote blocking the expression of IL-6 using MR16-1.

Treatment With MR16-1 + BMSCs Reduced the Protein Levels of IL-6 and TNF and Increased the Levels of BDNF, NGF, VEGF, and IGF-1 at the Lesion Site After SCI

There was a gradual decline in the protein levels of IL-6 and TNF in the control BMSCs alone group and MR16-1 alone group with time; however, these levels were significantly lower in the MR16-1 + BMSC cotreatment group than in the single treatment groups at each time point. Conversely, protein levels of BDNF, NGF, VEGF, and IGF-1 also decreased with time in the control single treatment groups (and were evidenced only by a low-density band at 1 and 7 days after SCI); levels of these trophic factors were maintained and were significantly higher in the MR16-1 + BMSC cotreatment group (Fig. 3).

The Death of Transplanted BMSCs Was Caused by Apoptosis

To establish the mechanism of transplanted BMSC death, we performed flow cytometry using Annexin V and PI on extracted GFP-positive cells from the injured spinal cords. Most of the transplanted BMSCs (GFP-positive cells) were Annexin V positive/PI negative at 7 days after transplantation in the control (BMSC alone) group (98.2% of GFP-positive cells; 16,909 ± 3,711 cells of the 17,215 ± 3,891 GFP-positive cells scored); this strongly suggests that the BMSCs die because of early apoptosis, as opposed to necrosis. Conversely, the rate of apoptotic BMSCs observed was significantly decreased (53.3% of GFP-positive cells; 12,178 ± 2,279 cells of the 20,809 ± 4,103 GFP-positive cells scored) in the MR16-1 + BMSC cotreatment group at the same time point after BMSC transplant (Fig. 4).

The positive area of TUNEL staining that colocalized with GFP positivity in the injured spinal cord was significantly decreased in the MR16-1 + BMSC cotreatment group compared with that in the control group (BMSCs alone) at 1 and 7 days after BMSC transplantation. At 14 days after BMSC transplantation, only small areas that were positive for both TUNEL and GFP were found in the MR16-1 + BMSC cotreatment and also the control group (Fig. 5A–E). The presence of apoptotic cells was further confirmed using electron microscopy, where cells with a segmented nucleus were seen more frequently in the control (BMSCs alone) group (Fig. 5F) than in the MR16-1 + BMSC cotreatment group (Fig. 5G).

The positive areas of caspase-3, -8, and -9 that colocalized with GFP positivity in the injured spinal cord were significantly decreased in the MR16-1 + BMSC cotreatment group compared with those in the control (BMSCs alone) group at 1 and 7 days after BMSC transplantation. At 14 days after transplantation, only small remnants of these positive areas were found in both groups (Fig. 6).

MR16-1 Treatment Increased the Expression of Akt and ERK1/2

Immunofluorescent staining and flow cytometry were performed to determine the expression of Akt and ERK1/2 (survival factors; mitogen-activated protein kinase pathway) after MR16-1 + BMSC cotreatment. The Akt-positive areas were extensive at 1 day after transplantation in both the MR16-1 + BMSC cotreatment and control (BMSCs alone) groups and decreased significantly at 7 and 14 days after transplantation. In contrast, the expression of ERK1/2 increased from 1 to 7 days after BMSC transplantation in the MR16-1 + BMSC cotreatment group but decreased from 1 to 14 days after BMSC transplantation in the control group. At 14 days after BMSC transplantation, ERK1/2-positive areas were still found in the MR16-1 + BMSC cotreatment group despite the uniform decrease evidenced from 7 to 14 days (Fig. 7A–F). In the flow cytometric analysis of extracted cells from the spinal cord of mice at 7 days after BMSC transplantation, the number of Akt-positive and ERK1/2-positive cells in the GFP-positive cell fraction was remarkably greater in the MR16-1 + BMSC cotreatment group (61.6%; 14,584 ± 3,583 cells and 75.1%; 17,780 ± 3,911 of GFP-positive

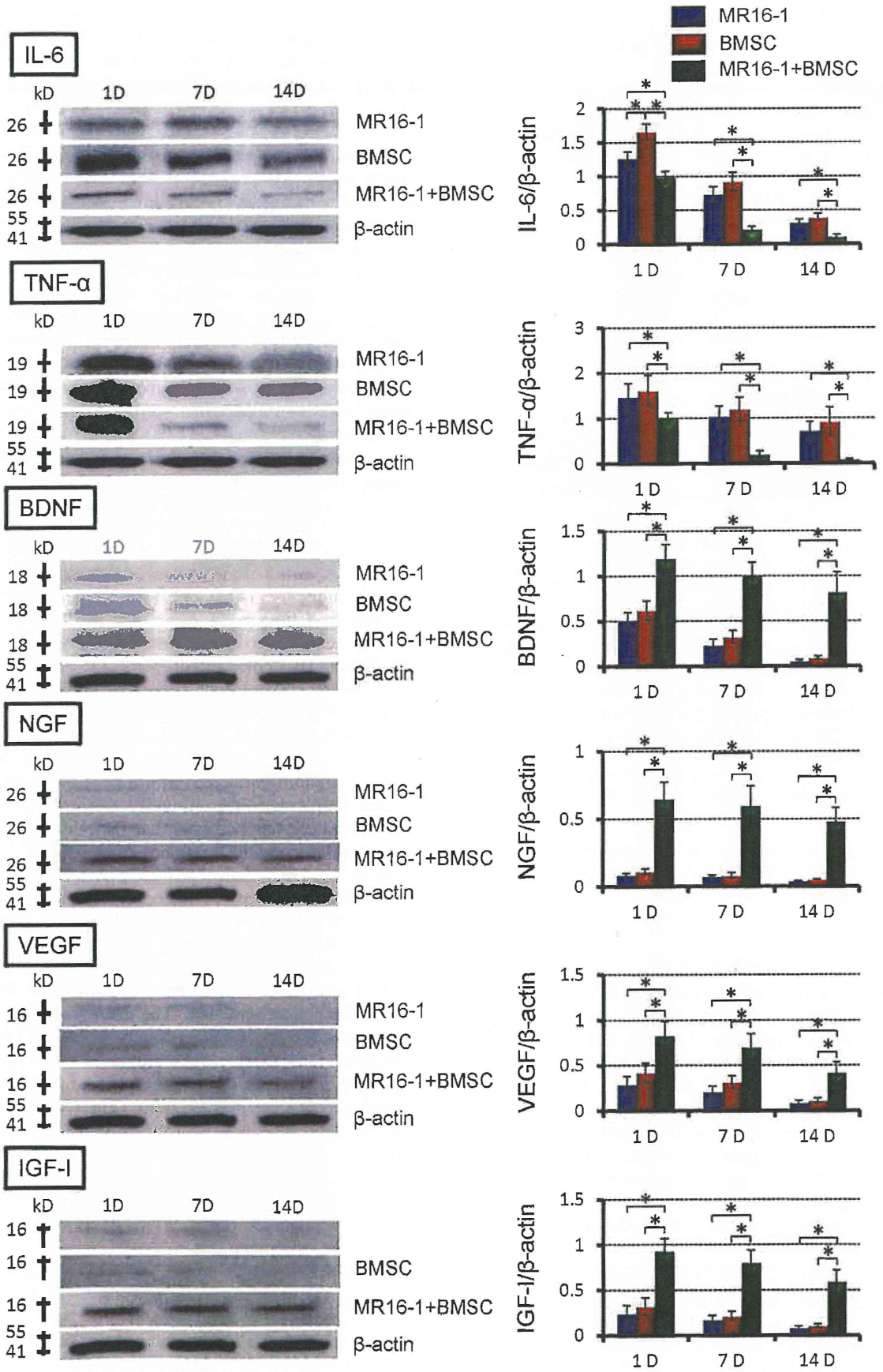

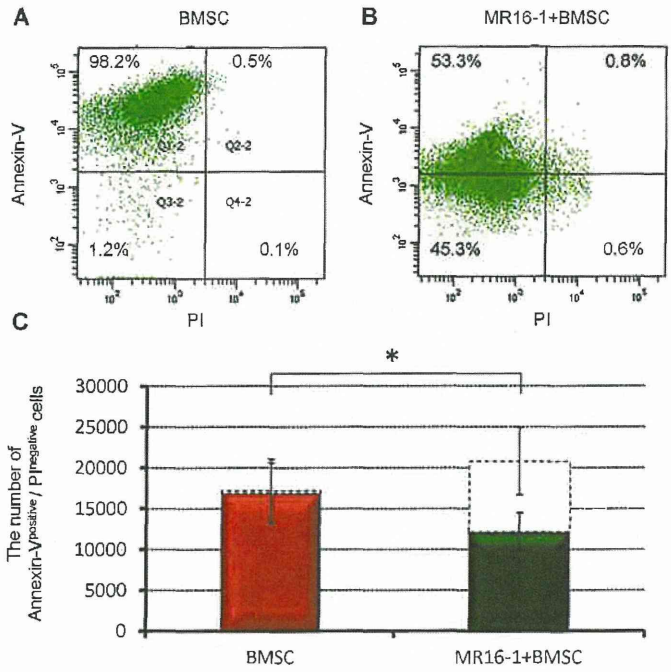

FIGURE 4. Cotreatment with MR16-1 protects transplanted bone marrow stromal cells (BMSCs) from undergoing apoptosis in the injured spinal cord assessed using Annexin V and propidium iodide (PI) staining. **(A, B)** Flow cytometry analysis after MR16-1 cotreatment. Flow cytometry using Annexin V and PI demonstrated the apoptotic mechanism of transplanted BMSC death. Almost all of transplanted BMSCs (green fluorescent protein [GFP]–positive cells) at 7 days after transplantation showed Annexin V positivity and PI negativity, indicating that the BMSCs died because of apoptosis but not necrosis. **(C)** Graph showing effects of MR16-1 cotreatment in preventing apoptosis of BMSCs at 3 days after BMSC transplantation. The dotted bars indicate total numbers of GFP-positive cells.

cells, respectively) versus those in the control group (7.0%; 1,205 ± 228 cells and 15.3%; 2,634 ± 552 of GFP-positive cells, respectively) (Fig. 7G–L).

DISCUSSION

MR16-1 is a neutralizing antibody for the IL-6R that competitively inhibits its binding to IL-6, thereby blocking IL-6R–mediated cell signaling. MR16-1 has a half-life of 3 days in mice and exhibits anti-inflammatory properties in rheumatoid arthritis (35) and SCI (26, 27). Recent studies have suggested that tissue sparing and functional recovery after MR16-1 treatment in mice with SCI are mediated by the IL-6/Janus kinase (Jak)/signal transducer and activator of transcription 3 (STAT3) signal transduction pathways (26), and that microglial functions associated with a decreased expression of recruiting inflammatory chemokines and an increased expression of granulocyte/macrophage colony-stimulating factor are also involved (27). A single MR16-1 treatment in mice with contusion SCI reduced interferon-γ (IFN-γ) and TNF levels (Th1 cytokines), with a parallel increase in IL-4 and IL-13 levels (Th2 cytokines) at the site of the spinal lesion; this was associated with the formation of alternatively activated M2 macrophages (28). Based on these reports and the data shown in the present study, we suggest that MR16-1 treatment immediately after SCI may promote the survival of BMSCs transplanted into the injured spinal cord and hence augment the improvements seen as a result of this cell transplantation intervention.

There are some reports that BMSCs have disappeared during 1 to 2 weeks after transplantation in the acute or subacute phase after injury because of the inflammatory reaction (14, 15). Immune cells rapidly invade contused spinal cord tissue after SCI, followed by inflammatory cells, including hematogenous macrophages and microglia, which are major components of the inflammatory pathology of SCI. The peak of activated microglia/macrophage present in the spinal cord is around 7 days after injury (36, 37). We found that the survival of BMSCs was greatest when the cells were transplanted 3 days after SCI, which is when numbers of inflammatory cells are still increasing in the contusion lesion (Figure, Supplemental Digital Content 2, http://links.lww.com/NEN/A503), and as also reported previously (14). Therefore, we determined that this was the optimal time point to perform BMSC transplantation to closely examine combinatorial effects of the BMSC transplant with MR16-1 cotreatment.

Bone marrow stromal cells release BDNF, VEGF, and cytokines such as IL-6, monocyte chemotactic protein 1, stromal cell–derived factor-1a (38), and IGF-1 (39). Neuroprotective properties of BMSCs have also been shown in coculture (9, 40, 41) and organotypic slice culture (42). Bone marrow stromal cell transplantation continually facilitates endogenous neurorestorative mechanisms that include a reduction of apoptotic cell death and the promotion of glial, neuronal, and blood vascular remodeling; indeed, BMSCs have been regarded as "a small molecular factory" of neuroprotective function (43). The present results demonstrate a decrease of IL-6 and TNF and the maintenance of BDNF, NGF, VEGF, and IGF-1 levels until 14 days after a combination of BMSC transplantation with MR16-1 cotreatment to an extent that is greater than that seen after BMSC transplantation alone. The decrease in levels of IL-6 may evidence the suppressive effect of MR16-1 treatment in stopping the overexpression and secretion of IL-6 in the injured spinal cord both from endogenous cells and also from the grafted BMSCs. The IL-6 blockade is also likely to be responsible for the decrease in levels of TNF present in the injured spinal cord possibly through inhibition of TNF production in astrocytes (26) because IL-6 regulates the expression and secretion of TNF (44). Furthermore, the relative overexpression of BDNF, NGF, VEGF, and IGF-1, which likely contributes to

FIGURE 3. Immunoblot analysis of cytokines and neurotrophic factors after MR16-1 treatment. Western blotting samples from the MR16-1 + bone marrow stromal cells (BMSCs) cotreatment group showed significantly lower levels of interleukin 6 (IL-6) and tumor necrosis factor (TNF) versus the BMSCs or MR16-1 alone groups, whereas brain-derived neurotrophic factor (BDNF), nerve growth factor (NGF), vascular endothelial growth factor (VEGF), and insulin-like growth factor 1 (IGF-1) levels were significantly higher in the MR16-1 cotreatment group versus the BMSCs or MR16-1 alone groups at 1, 7, and 14 days after BMSC transplantation.

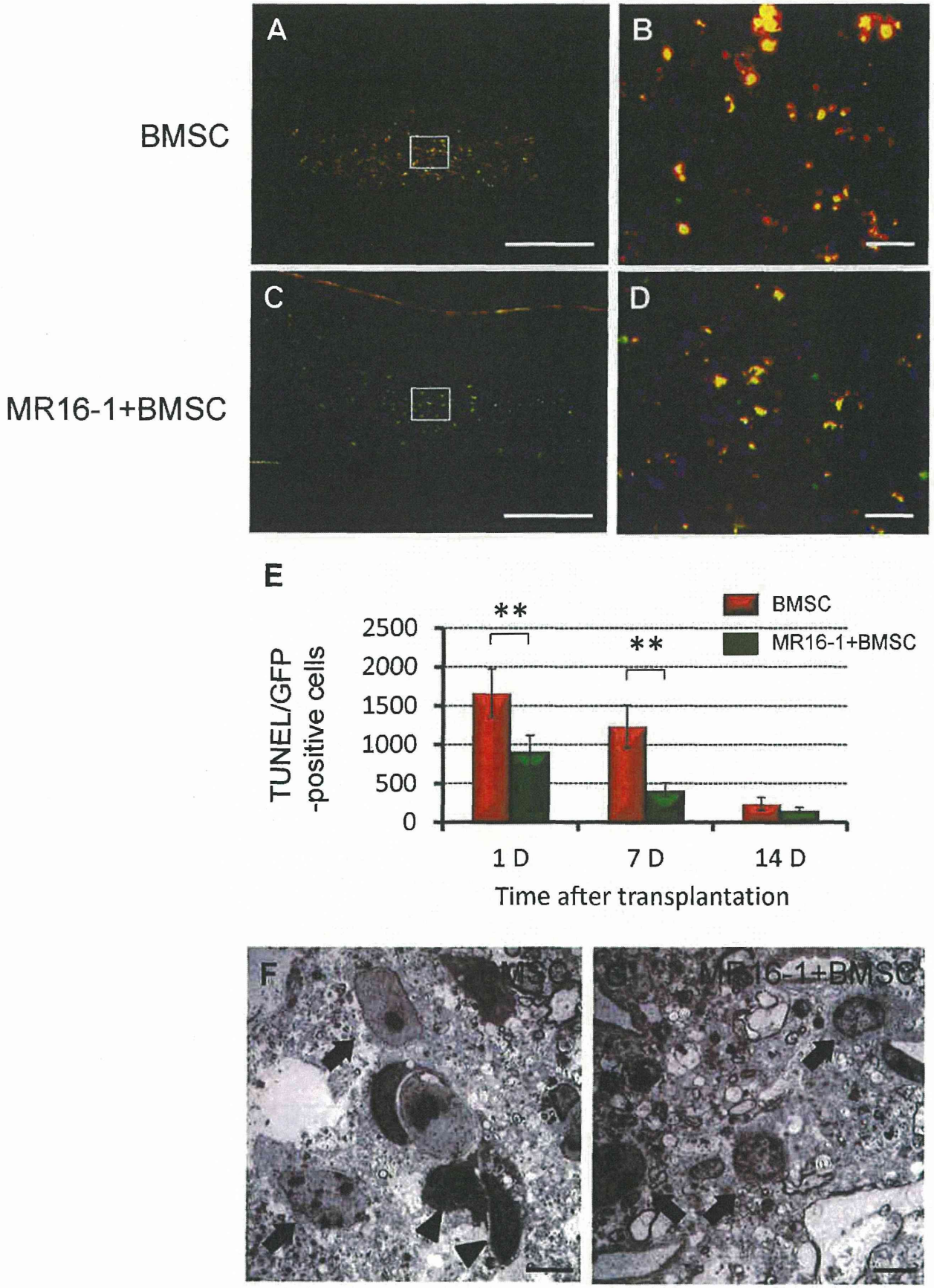

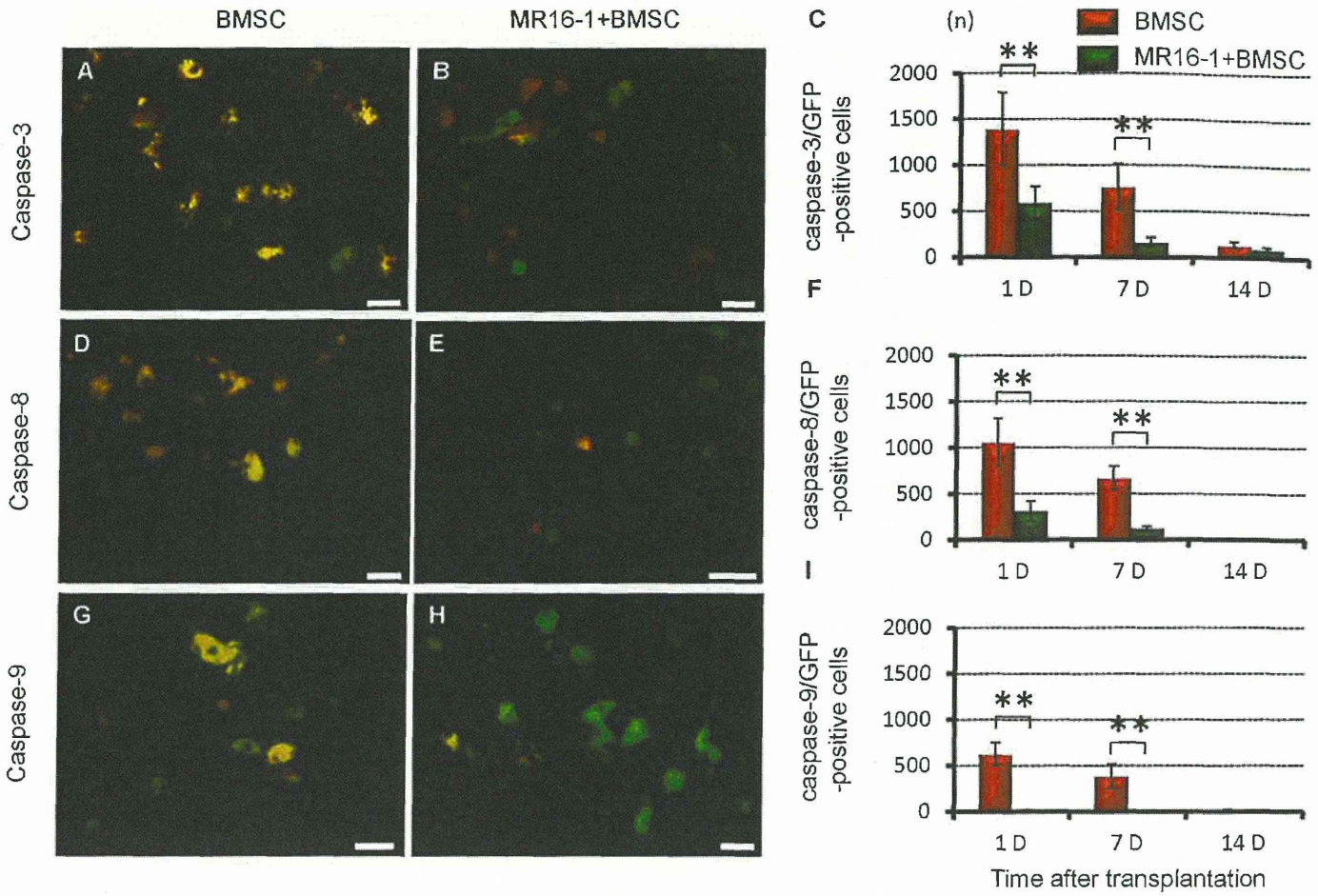

FIGURE 6. MR16-1 cotreatment protects transplanted bone marrow stromal cells (BMSCs) from undergoing apoptosis in the injured spinal cord, as assessed by immunolocalization of proapoptotic caspases. **(A–I)** Representative immunofluorescence staining showing the colocalization of caspase-3 **(A, B)**, -8 **(D, E)**, and -9 **(G, H)** (red) with green fluorescent protein (GFP)–positive BMSCs (green) in the injured spinal cord epicenter. In **(C, F, and I)**, the prevalence of GFP/caspase-3, -8, or -9 double-positive cells was significantly reduced in the MR16-1 + BMSC cotreatment group versus the control group (BMSCs alone) group at 1 and 7 days after BMSC transplantation. Scale bar = **(A–H)** 25 μm. ** $p < 0.01$.

the higher locomotion improvement found in the MR16-1 cotreatment group, depends on the higher survival rate and activation of the grafted BMSCs by the blockade of IL-6.

The adult CNS, particularly the injured CNS, may provide a relatively nonpermissive environment for transplanted BMSCs and other stem cells. Even under the best circumstances, levels of cell survival in the injured CNS have been estimated to be near 10% (45, 46), and few transplanted cells differentiate into mature neuronal phenotypes (47, 48). Bone marrow stromal cells from autologous donor sources have been reported to attenuate adaptive immune reactions in vitro and in vivo (49). These attributes should promote their long-term survival after transplantation to the CNS. To our surprise, previous researchers have documented that even transplantation of BMSCs to the normal noninjured adult brain elicits an inflammatory response, with complete rejection of the BMSCs by 14 days (17); this also can induce inflammatory reactions from host cells (18). The histologic evidence in these studies suggested that BMSCs were rejected by an inflammatory response related to microglia/macrophage activation. Similarly,

FIGURE 5. MR16-1 cotreatment protects transplanted bone marrow stromal cells (BMSCs) from undergoing apoptosis in the injured spinal cord, as assessed using terminal deoxynucleotidyl transferase (TdT)–mediated dUTP-biotin nick end labeling (TUNEL) and electron microscopy. **(A–D)** Representative immunofluorescence staining of sagittal **(A, C)** and axial **(B, D)** sections showing the colocalization of TUNEL staining (red) with green fluorescent protein (GFP)–positive BMSCs (green) in the injured spinal cord epicenter at 7 days after BMSC transplantation. **(E)** The prevalence of TUNEL/GFP-positive apoptotic BMSCs was significantly reduced in the MR16-1 + BMSC cotreatment group versus that in the control group (BMSCs alone) at 1 and 7 days after BMSC transplantation. **(F, G)** Using electron microscopy, apoptotic BMSCs (arrowhead) were detected in the injured spinal cord epicenter at 7 days after transplantation. Higher numbers of apoptotic BMSCs were detected in the control group **(F)** than in the MR16-1 + BMSC cotreatment group **(G)**. Arrow: surviving BMSCs. Scale bars = **(A, C)** 500 μm; **(B, D, F, G)** 25 μm. * $p < 0.01$.

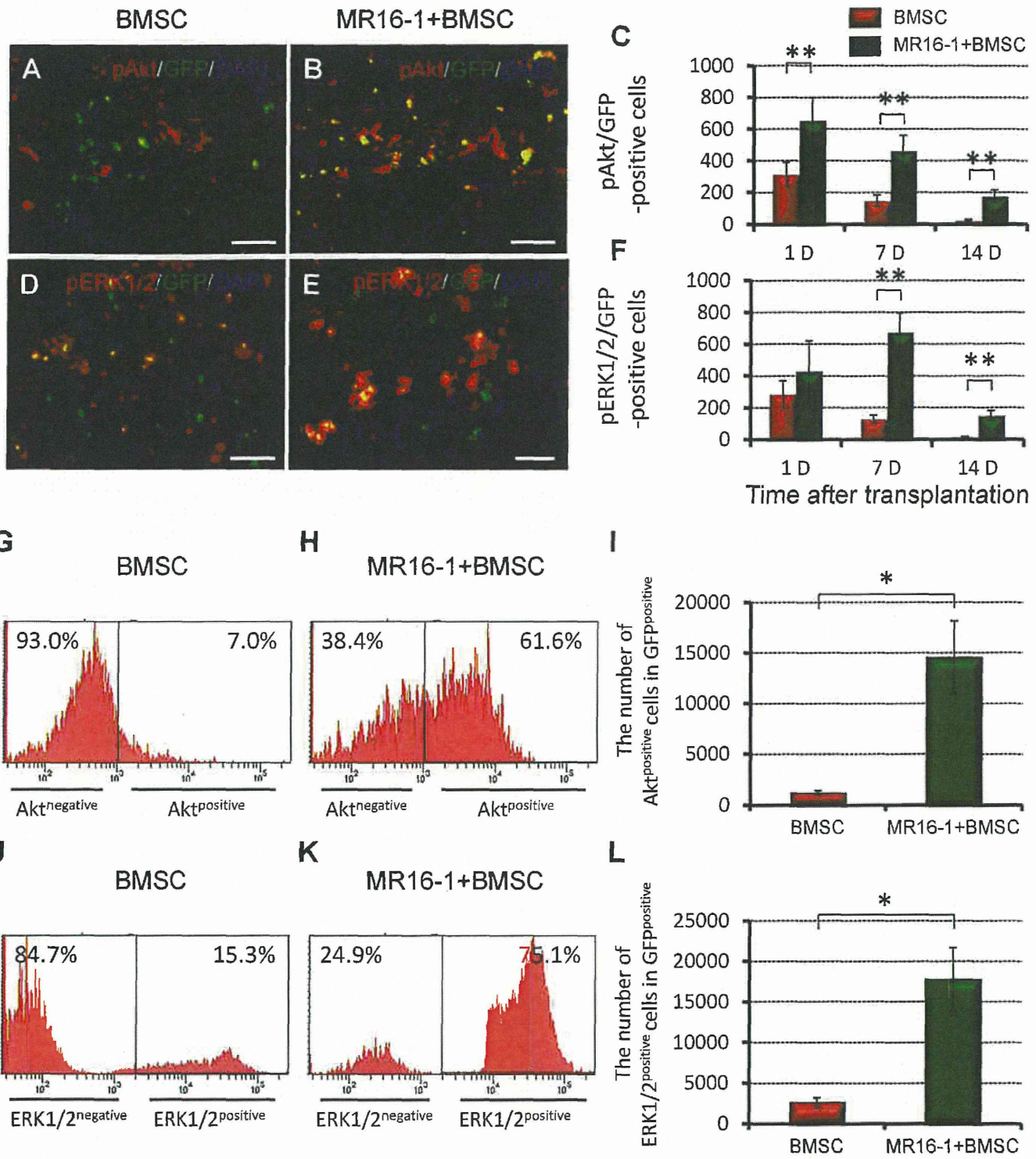

FIGURE 7. MR16-1 cotreatment protects transplanted bone marrow stromal cells (BMSCs) from undergoing apoptosis in the injured spinal cord, as assessed by immunopositivity for the prosurvival pAkt and pERK1/2 signaling pathways. (**A–F**) Representative immunofluorescence stainings show the colocalization of pAkt (**A, B**) and ERK1/2 (**D, E**) (red) with green fluorescent protein (GFP)–positive BMSCs (green) in the injured spinal cord epicenter at 7 days after transplantation. The prevalence of pAkt- and pERK1/2/GFP-positive BMSCs was significantly increased in the MR16-1 + BMSC cotreatment group versus the control group (BMSCs alone) at 1 and 7 days after transplantation (**C, F**). (**G–L**) Representative histograms of flow cytometry data at 7 days after cotreatment with MR16-1 + BMSC transplantation versus the control (BMSCs alone) (**G, J**) and MR16-1–treated (**H, K**) groups. (**I, L**) Numbers of Akt-positive (**I**) and ERK1/2-positive (**L**) cells in the GFP-positive BMSCs are shown in the graphs. MR16-1 treatment promoted an increased population of Akt- and ERK1/2-positive BMSCs. Scale bars = **(A, B, D, E)** 50 μm.

inflammatory and immune responses after transplantation of BMSCs have also been observed in other organs and tissues, such as the heart (50, 51), kidney (52), and in inflammatory bowel disease (53). In these other areas of research, the causes of BMSC death after transplantation are multifactorial and influenced by host inflammatory response mediators, deficiency of nutrients, oxidative stress, and others factors, where apoptosis has been implicated as the main contributor in a massive loss of donor cells (54). Therefore, we hypothesized that low survival rates of transplanted BMSCs after transplantation into SCI might arise through BMSCs undergoing apoptosis because the transplanted cells are exposed to severe conditions in the injured CNS. At least in vitro, the Fas ligand–activated pathway in BMSCs has also been demonstrated as an extrinsic induction of apoptotic cell death (55). In the present study, flow cytometry using Annexin V and PI showed that almost all BMSC deaths were caused by apoptosis but not necrosis. In addition, both TUNEL staining and electron microscopy detected apoptotic BMSCs, with GFP positivity colocalized with anti–caspase-3, -8, and -9 immunopositivity from 1 day after transplantation. These findings suggest that induction of apoptosis of BMSCs could involve both intrinsic and extrinsic pathways—somewhat similar to the inflammatory and immune responses that have been reported after transplantation of BMSCs into other organs (50, 51, 54). Interestingly, all analysis of apoptotic cell death in the present study indicated that MR16-1 cotreatment immediately after injury prevented apoptosis of transplanted BMSCs.

Concomitant with activation of apoptotic pathways, survival signaling pathways are activated. Among them, the phosphatidylinositol 3-kinase (PI3K)/Akt pathway is activated by many stimuli of apoptosis and plays a critical role in balancing levels of apoptosis (56). Although the ERK pathway is attributed to a survival response for many cell types, ERK activation is thought to contribute to apoptosis as well (50). In vitro studies have reported that enhanced expression of ERK/Akt in BMSCs increases their survival in conditions of hypoxia (57), whereas in vivo studies have demonstrated that increased Akt activity in BMSCs protects them from hypoxia secondary to ischemia (58). Our results show that MR16-1 cotreatment suppressed apoptosis in transplanted BMSCs and simultaneously promoted an increased population of Akt and ERK1/2-positive BMSCs compared with the control condition, as assessed by both immunofluorescence staining and flow cytometric analysis. This suggests that the Akt/ERK1/2 pathways may play an important role in protecting BMSCs from undergoing apoptosis after their transplantation into the injured spinal cord and that this has been augmented by the blockade of IL-6 signaling by the MR16-1 treatment. On the other hand, adequate expression of IL-6 is both necessary and sufficient for enhanced BMSC proliferation, differentiation, and protection from apoptosis (59). Interleukin 6 has been implicated as a potent mediator of numerous biologic processes, including differentiation, proliferation, and apoptosis through the gp130/Jak/STAT pathway (60). We recently reported that a single MR16-1 treatment (i.e. in the absence of cell transplants) to block IL-6 signaling suppressed IFN-γ expression by neutrophils and increased IL-4 expression by activated microglia in a mouse SCI model, promoting the formation of alternatively activated M2 macrophages (28). In addition, we have reported that the acute transplantation of BMSCs after SCI in mice also modified the inflammatory environment by shifting the macrophage phenotype from M1 to M2 (10). Other researchers have similarly reported the alternative activation of microglia/macrophages after transplantation of BMSCs in a mouse model of brain ischemia (39). The ability of trophic factors to promote survival have been attributed, at least in part, to the PI3K/Akt kinase cascade, and it is known that many physiologic stimuli are capable of inducing Akt kinase activity, primarily in a PI3K-dependent manner (56). The results presented here, and previously by others (10, 28, 39), concerning the survival of BMSC transplants after MR16-1 cotreatment may suggest the following sequence of events: 1) the blockade of IL-6 signaling suppressed the expression of Th1 cytokines and promoted Th2 cytokines, which had anti-inflammatory and anti-immune responses and neuroprotective effects related to promotion of the alternative activation of microglia/macrophages; 2) transplanted BMSCs were activated by the stress signal resulting from severe vascular, cellular, and biochemical events after SCI despite MR16-1 treatment; 3) the activated BMSCs upregulated the expression of BDNF, NGF, VEGF, IGF-1, which act as anti-immune, antiapoptotic, and neuroprotective factors; 4) the activated BMSCs caused alternative activation of microglia/macrophage either by secretion of paracrine factors or by cell-cell contacts; 5) the alternatively activated microglia/macrophage further increased the expression of cell survival or neuroprotective factors; and 6) treatment with MR16-1 enhanced the survival of transplanted BMSCs in addition to promoting the formation of alternative microglia/macrophages. The overall effect of a combination MR16-1 cotreatment with transplantation of BMSCs was therefore to rescue neuronal cells and axons through modulation of the inflammatory/immune responses and decreased apoptosis, which resulted in increased neurologic function.

Altogether, our findings provide a new strategy to increase the survival rate of transplanted BMSCs, and probably other stem cells, which increases their immunomodulatory and neuroprotective effect, and may enable their capacity to undergo neural differentiation. Because a humanized version of MR16-1 is already available for the treatment of rheumatoid arthritis and approved by the US Food and Drug Administration (Actemra) and the European Union (RoActemra), suppressing the acute inflammation seen after SCI and also cell transplantation procedures by MR16-1 treatment provides an applicable method to increase the efficiency of BMSC transplantation in the clinics. Our work also suggests a treatment strategy for repairing degenerative central and peripheral nervous system injuries in their early stages.

ACKNOWLEDGMENTS

The authors thank Mr. Hitoshi Takagi and Mrs. Junko Yamamoto of the Life Science Research Laboratory, University of Fukui, Division of Bioresearch, for advice with respect to the confocal microscopy and flow cytometry experiments.

REFERENCES

1. Ramer MS, Harper GP, Bradbury EJ. Progress in spinal cord research—A refined strategy for the International Spinal Research Trust. Spinal Cord 2000;38:449–72

2. Blight AR. Miracles and molecules—Progress in spinal cord repair. Nat Neurosci 2002;5:1051–54
3. Hausmann ON. Posttraumatic inflammation following spinal cord injury. Spinal Cord 2003;41:369–78
4. Selzer ME. Promotion of axonal regeneration in the injured CNS. Lancet Neurol 2003;2:157–66
5. Thuret S, Moon LD, Gage FH. Therapeutic interventions after spinal cord injury. Nat Rev Neurosci 2006;7:628–43
6. Parr AM, Tator CH, Keating A. Bone marrow–derived mesenchymal stromal cells for the repair of central nervous system injury. Bone Marrow Transplant 2007;40:609–19
7. Tetzlaff W, Okon EB, Karimi-Abdolrezaee S, et al. A systematic review of cellular transplantation therapies for spinal cord injury. J Neurotrauma 2011;28:1611–82
8. Wright KT, El Masri W, Osman A, et al. Concise review: Bone marrow for the treatment of spinal cord injury: Mechanisms and clinical applications. Stem Cells 2011;29:169–78
9. Wright KT, El Masri W, Osman A, et al. Bone marrow stromal cells stimulate neurite outgrowth over neural proteoglycans (CSPG), myelin associated glycoprotein and Nogo-A. Biochem Biophys Res Commun 2007;354:559–66
10. Nakajima H, Uchida K, Guerrero AR, et al. Transplantation of mesenchymal stem cells promotes an alternative pathway of macrophage activation and functional recovery after spinal cord injury. J Neurotrauma 2012;29:1614–25
11. Akiyama Y, Radtke C, Kocsis JD. Remyelination of the rat spinal cord by transplantation of identified bone marrow stromal cells. J Neurosci 2002; 22:6623–30
12. Zhao ZM, Li HJ, Liu HY, et al. Intraspinal transplantation of CD34+ human umbilical cord blood cells after spinal cord hemisection injury improves functional recovery in adult rats. Cell Transplant 2004;13:113–22
13. Hofstetter CP, Schwarz EJ, Hess D, et al. Marrow stromal cells form guiding strands in the injured spinal cord and promote recovery. Proc Natl Acad Sci USA 2002;99:2199–204
14. Nandoe Tewarie RD, Hurtado A, Ritfeld GJ, et al. Bone marrow stromal cells elicit tissue sparing after acute but not delayed transplantation into the contused adult rat thoracic spinal cord. J Neurotrauma 2009;26: 2313–22
15. Ide C, Nakai Y, Nakano N, et al. Bone marrow stromal cell transplantation for treatment of subacute spinal cord injury in the rat. Brain Res 2010;1332:32–47
16. Wu W, Zhao H, Xie B, et al. Implanted spike wave electric stimulation promotes survival of the bone marrow mesenchymal stem cells and functional recovery in the spinal cord injured rats. Neurosci Lett 2011; 491:73–78
17. Coyne TM, Marcus AJ, Woodbury D, et al. Marrow stromal cells transplanted to the adult brain are rejected by an inflammatory response and transfer donor labels to host neurons and glia. Stem Cells 2006;24: 2483–92
18. Coyne TM, Marcus AJ, Reynolds K, et al. Disparate host response and donor survival after the transplantation of mesenchymal or neuroectodermal cells to the intact rodent brain. Transplantation 2007;84:1507–16
19. Nesic O, Xu GY, McAdoo D, et al. IL-1 receptor antagonist prevents apoptosis and caspase-3 activation after spinal cord injury. J Neurotrauma 2001;18:947–56
20. Chen KB, Uchida K, Nakajima H, et al. Tumor necrosis factor-α antagonist reduces apoptosis of neurons and oligodendroglia in rat spinal cord injury. Spine 2011;36:1350–58
21. Gruol DL, Nelson TE. Physiological and pathological roles of interleukin-6 in the central nervous system. Mol Neurobiol 1997;15:307–39
22. Van Wagoner NJ, Benveniste EN. Interleukin-6 expression and regulation in astrocytes. J Neuroimmunol 1999;100:124–39
23. Bethea JR, Dietrich WD. Targeting the host inflammatory response in traumatic spinal cord injury. Curr Opin Neurol 2002;15:355–60
24. Chai Z, Gatti S, Toniatti C, et al. Interleukin (IL)-6 gene expression in the central nervous system is necessary for fever response to lipopolysaccharide or IL-1 beta: A study on IL-6–deficient mice. J Exp Med 1996; 183:311–16
25. Cafferty WB, Gardiner NJ, Das P, et al. Conditioning injury-induced spinal axon regeneration fails in interleukin-6 knockout mice. J Neurosci 2004;24:4432–43
26. Okada S, Nakamura M, Mikami Y, et al. Blockade of interleukin-6 receptor suppresses reactive astrogliosis and ameliorates functional recovery in experimental spinal cord injury. J Neurosci Res 2004;76: 265–76
27. Mukaino M, Nakamura M, Yamada O, et al. Anti-IL-6-receptor antibody promotes repair of spinal cord injury by inducing microglia-dominant inflammation. Exp Neurol 2010;224:403–14
28. Guerrero AR, Uchida K, Nakajima H, et al. Blockade of interleukin-6 signaling inhibits the classic pathway and promotes an alternative pathway of macrophage activation after spinal cord injury in mice. J Neuroinflammation 2012;9:40
29. Tamura T, Udagawa N, Takahashi N, et al. Soluble interleukin-6 receptor triggers osteoclast formation by interleukin 6. Proc Natl Acad Sci U S A 1993;90:11924–28
30. Soleimani M, Nadri S. A protocol for isolation and culture of mesenchymal stem cells from mouse bone marrow. Nat Protoc 2009;4:102–6
31. Scheff SW, Rabchevsky AG, Fugaccia I, et al. Experimental modeling of spinal cord injury: Characterization of a force-defined injury device. J Neurotrauma 2003;20:179–93
32. Basso DM, Fisher LC, Anderson AJ, et al. Basso Mouse Scale for locomotion detects differences in recovery after spinal cord injury in five common mouse strains. J Neurotrauma 2006;23:635–59
33. Saiwai H, Ohkawa Y, Yamada H, et al. The LTB4-BLT1 axis mediates neutrophil infiltration and secondary injury in experimental spinal cord injury. Am J Pathol 2010;176:2352–66
34. Stirling DP, Yong VW. Dynamics of the inflammatory response after murine spinal cord injury revealed by flow cytometry. J Neurosci Res 2008;86:1944–58
35. Choy EH, Isenberg DA, Garrood T, et al. Therapeutic benefit of blocking interleukin-6 activity with an anti–interleukin-6 receptor monoclonal antibody in rheumatoid arthritis: A randomized, double-blind, placebo-controlled, dose-escalation trial. Arthritis Rheum 2002;46:3143–50
36. Popovich PG, Wei P, Stokes BT. Cellular inflammatory response after spinal cord injury in Sprague-Dawley and Lewis rats. J Comp Neurol 1997;377:443–64
37. Jones TB, McDaniel EE, Popovich PG. Inflammatory-mediated injury and repair in the traumatically injured spinal cord. Curr Pharm Des 2005; 11:1223–36
38. Neuhuber B, Timothy Himes B, Shumsky JS, et al. Axon growth and recovery of function supported by human bone marrow stromal cells in the injured spinal cord exhibit donor variations. Brain Res 2005;1035:73–85
39. Ohtaki H, Ylostalo JH, Foraker JE, et al. Stem/progenitor cells from bone marrow decrease neuronal death in global ischemia by modulation of inflammatory/immune responses. Proc Natl Acad Sci USA 2008;105: 14638–43
40. Wu S, Suzuki Y, Ejiri Y, et al. Bone marrow stromal cells enhance differentiation of cocultured neurosphere cells and promote regeneration of injured spinal cord. J Neurosci Res 2003;72:343–51
41. Isele NB, Lee HS, Landshamer S, et al. Bone marrow stromal cells mediate protection through stimulation of PI3-K/Akt and MAPK signaling in neurons. Neurochem Int 2007;50:243–50
42. Kamei N, Tanaka N, Oishi Y, et al. Bone marrow stromal cells promoting corticospinal axon growth through the release of humoral factors in organotypic cocultures in neonatal rats. J Neurosurg Spine 2007;6: 412–19
43. Li Y, Chopp M. Marrow stromal cell transplantation in stroke and traumatic brain injury. Neurosci Lett 2009;456:120–23
44. Klusman I, Schwab ME. Effects of proinflammatory cytokines in experimental spinal cord injury. Brain Res 1997;762:173–84
45. Zompa EA, Cain LD, Everhart AW, et al. Transplant therapy: Recovery of function after spinal cord injury. J Neurotrauma 1997;14: 479–506
46. Vescovi AL, Snyder EY. Establishment and properties of neural stem cell clones: Plasticity in vitro and in vivo. Brain Pathol 1999;9:569–98
47. Svendsen CN, Clarke DJ, Rosser AE, et al. Survival and differentiation of rat and human epidermal growth factor-responsive precursor cells following grafting into the lesioned adult central nervous system. Exp Neurol 1996;137:376–88
48. Park KI, Liu S, Flax JD, et al. Transplantation of neural progenitor and stem cells: Developmental insights may suggest new therapies for spinal cord and other CNS dysfunction. J Neurotrauma 1999;16:675–87

49. Le Blanc K. Immunomodulatory effects of fetal and adult mesenchymal stem cells. Cytotherapy 2003;5:485–89
50. Zhuang S, Schnellmann RG. A death-promoting role for extracellular signal-regulated kinase. J Pharmacol Exp Ther 2006;319:991–97
51. Robey TE, Saiget MK, Reinecke H, et al. Systems approaches to preventing transplanted cell death in cardiac repair. J Mol Cell Cardiol 2008;45:567–81
52. Hughes A, Mohanasundaram D, Kireta S, et al. Insulin-like growth factor-II (IGF-II) prevents proinflammatory cytokine-induced apoptosis and significantly improves islet survival after transplantation. Transplantation 2013;95:671–78
53. Luna J, Masamunt MC, Lawrance IC, et al. Mesenchymal cell proliferation and programmed cell death: Key players in fibrogenesis and new targets for therapeutic intervention. Am J Physiol Gastrointest Liver Physiol 2011;300:G703–8
54. Haider HKh, Ashraf M. Preconditioning and stem cell survival. J Cardiovasc Transl Res 2010;3:89–102
55. Mazar J, Thomas M, Bezrukov L, et al. Cytotoxicity mediated by the Fas ligand (FasL)-activated apoptotic pathway in stem cells. J Biol Chem 2009;284:22022–28
56. Datta SR, Brunet A, Greenberg ME. Cellular survival: A play in three Akts. Genes Dev 1999;13:2905–27
57. Yin Q, Jin p, Liu X, et al. SDF-1α inhibits hypoxia and serum deprivation-induced apoptosis in mesenchymal stem cells through PI3K/Akt and ERK1/2 signaling pathways. Mol Biol Rep 2011;38:9–16
58. Mangi AA, Noiseux N, Kong D, et al. Mesenchymal stem cells modified with Akt prevent remodeling and restore performance of infarcted hearts. Nat Med 2003;9:1195–1201
59. Pricola KL, Kuhn NZ, Haleem-Smith H, et al. Interleukin-6 maintains bone marrow-derived mesenchymal stem cell stemness by an ERK1/2-dependent mechanism. J Cell Biochem 2009;108:577–88
60. Heinrich PC, Behrmann I, Müller-Newen G, et al. Interleukin-6-type cytokine signalling through the gp130/Jak/STAT pathway. Biochem J 1998;334:297–314

Spine

SPINE Volume 38, Number 1, pp E21–E27

CLINICAL CASE SERIES

The Cutoff Amplitude of Transcranial Motor-Evoked Potentials for Predicting Postoperative Motor Deficits in Thoracic Spine Surgery

Akio Muramoto, MD,* Shiro Imagama, MD, PhD,* Zenya Ito, MD, PhD,* Norimitsu Wakao, MD, PhD,† Kei Ando, MD, PhD,* Ryoji Tauchi, MD, PhD,* Kenichi Hirano, MD,‡ Hiroki Matsui, MD,* Tomohiro Matsumoto, MD,* Yukihiro Matsuyama, MD, PhD§ and Naoki Ishigro, MD, PhD*

Study Design. Prospective clinical study of intraoperative transcranial motor-evoked potentials (TcMEP) amplitudes and postoperative motor deficits.

Objective. To determine the cutoff amplitude during intraoperative TcMEP monitoring for predicting postoperative motor deficits after thoracic spine surgery.

Summary of Background Data. Several alarm points when monitoring with TcMEP have been advocated, but there have been no reports on an actual cutoff amplitude of TcMEP for predicting the occurrence of postoperative motor deficits.

Methods. Among 80 consecutive surgical cases, 28 had a deterioration in TcMEP amplitude in at least 1 monitored muscle during surgery. We examined intraoperative electrophysiological changes and postoperative motor deficits in 270 monitorable muscles in those 28 patients. Through receiver operating characteristic curve analysis, we identified the cutoff amplitudes at the intraoperative point of deterioration and at the end of surgery for predicting postoperative motor deficits in both relative and absolute values.

Results. The relative and the absolute cutoff amplitudes of TcMEP at the intraoperative point of deterioration and at the end of thoracic spine surgery were 12% of control amplitude and 1.9 μV and 25% of control amplitude and 3.6 μV, respectively. Sensitivity/specificity for those cutoff points are 88%/64%, 69%/83%, 90%/64%, and 70%/82%, respectively.

Conclusion. We determined the cutoff amplitude for predicting postoperative motor deficits in thoracic spine surgery. The results may help establish the alarm criteria for thoracic spine surgery.

Key words: TcMEP, amplitude, absolute value, postoperative motor deficits, thoracic surgery. **Spine 2013;38:E21–E27**

Surgical procedures involving the thoracic spine, which include resection of intra- and extramedullary tumors, correction of deformities, and decompression and corrective procedures due to stenosis in cases of ossification of the posterior longitudinal ligament (OPLL) or ossification of the yellow ligament, are technically demanding and carry a high risk of postoperative motor deficit.[1,2] Previous reports clearly demonstrated that a multimodal approach to monitoring is essential for thoracic spine surgery in order to confirm the functional integrity of the entire spinal cord.[3,4] Among many monitoring modalities, transcranial motor-evoked potential (TcMEP) is most effective for corticospinal tract monitoring because it is easy to perform and has both high sensitivity and specificity.[5–7] Although the general method of stimulation and recording is widely agreed upon, the interpretation of TcMEP response remains controversial. During the past decade, different warning criteria for TcMEP monitoring have been proposed.[8,9] In Japan, a nationwide, prospective multicenter study has been conducted using a standard of 70% or greater decrease in amplitude. However, there have been no studies presenting a scientifically established cutoff amplitude that best determines when postoperative motor deficits will occur.

The purpose of this article was to establish cutoff amplitudes of TcMEP that indicates postoperative motor deficits at the intraoperative point of deterioration and at the end of surgery. To determine the ideal cutoff points, we conducted a prospective study involving 12 major lower extremity muscles in each patient and evaluated the TcMEP amplitude as a relative value in percentage of the baseline amplitude and an absolute value in microvolts.

From the *Department of Orthopedic Surgery, Nagoya University School of Medicine, Nagoya, Aichi, Japan; †Department of Orthopedic Surgery, Aichi Medical University, Aichi-gun, Aichi Japan; ‡Department of Orthopedic Surgery, Japanese Red Cross Nagoya First Hospital, Nakamura-ku, Japan; §Department of Orthopedic Surgery, Hamamatsu University School of Medicine, Hamamatsu, Japan.

Acknowledgment date: August 22, 2012. First revision date: September 30, 2012. Acceptance date: October 15, 2012.

The device(s)/drug(s) is/are FDA approved or approved by corresponding national agency for this indication.

No funds were received in support of this work.

No relevant financial activities outside the submitted work.

Address correspondence and reprint requests to Shiro Imagama, MD, PhD, Department of Orthopedic Surgery, Nagoya University Graduate School of Medicine, 65 Tsurumai Showa-ward, Nagoya, Aichi 466-8550, Japan; E-mail: si1222@b-star.jp

DOI: 10.1097/BRS.0b013e3182796b15

PATIENTS AND METHODS

Patient Selection and Neurological Evaluation

From June 2009 through January 2012, 80 consecutive thoracic spine surgery cases performed under intraoperative neurophysiological monitoring with TcMEP at our hospital were prospectively reviewed. Four cases, from which any monitorable baseline TcMEP from any lower extremity muscles were obtained, were excluded from the study. Preoperative motor status itself was not included in the exclusion criteria, but 3 of these 4 patients had severe neurological compromise. Seventy-six cases demonstrated acceptable baseline TcMEP responses at least from 1 muscle. We considered them monitorable and included them in this study. Of these, 43 cases showed preoperative motor deficits. Comorbidities were not in the exclusion criteria. There were 2 cases of thoracic lesion of metastatic tumor. Other cases did not have any lethal comorbidities.

A postoperative motor deficit was defined as a 1-point or greater decrease in the manual muscle test on the most immediate check after return to the recovery room compared with the preoperative motor status.

Anesthetic Management

Because benzodiazepine suppresses latency and amplitude, it was used minimally, if at all, as a preanesthetic medication. Propofol (3–4 mg/kg), fentanyl (2 mg/kg), and vecuronium (0.12–0.16 mg/kg) were administered for induction, and anesthesia was maintained using propofol (50–100 μg/kg/min), fentanyl (1–2.5 μg/kg/h), and vecuronium (0.01–0.04 mg/kg/h). Concomitant hypotensive anesthesia was given, as appropriate, by continuously administering PGE1 and a short-acting β1 blocker (landiolol). We always maintain our patients in a normothermic state, and should intraoperative spinal damage occur, the patient's temperature is raised. The anesthesiologist maintains end-tidal CO_2 in the reference range throughout surgery.

Stimulating and Recording Methods

We used a MS120B (Nihon Kohden, Tokyo, Japan) to perform transcranial stimulation. The stimulation parameters were 5 stimuli in a row, with 2 ms interstimulus intervals, constant biphasic current of 200 mA for a 500-μs duration, 50–1000 Hz filter, and 100 ms epoch time with 20 or less recorded signal responses. The stimulated point was 2 cm anterior and 3 cm lateral from the Cz (International 10–20 System) location over the cerebral cortex motor area (left: anode, right: cathode). Using the Neuromaster MEE-1000 ver. 04.12 (Nihon Kohden, Japan), which is expandable to 32 channels, we recorded muscle action potentials from the upper and lower extremities *via* a pair of needle electrodes 3 to 5 cm apart. We used the deltoid and hypothenar muscles bilaterally as controls and bilateral adductor longus, quadriceps femoris, hamstrings, tibialis anterior, gastrocnemius, abductor hallucis, and anal sphincter muscles as the target muscles. We performed multimodality monitoring in all cases. In particular, we combined Br-SCEP (D-wave) and somatosensory-evoked potentials (SSEP). In addition, free-running electromyograms from these muscles were monitored throughout the operation.

Monitoring and Alert Parameters

The TcMEP baseline value was taken immediately after the documented surgical exposure of the spine but before any decompression or instrumentation. Waiting until this point to take the baseline measurement also reduced the effects on TcMEP responses because of body and spinal cord temperature changes occurring with exposure. Final TcMEP testing was recorded at the end of wound closure. These data points included TcMEP peak-to-peak amplitude measurements in microvolts. Signals were rechecked after surgical exposure, decompression, tumor resection, and instrumentation, and the surgeons were informed of any acute change in the TcMEP responses. A 70% or greater loss in TcMEP amplitude in 1 or more muscles was considered a possibly significant neurological injury. If a 70% or greater decrease in TcMEP was accompanied with a significant decrease in D-waves or SSEPs, the surgeon reviewed the context of the alert in terms of the stage of the procedure and what was occurring within the operative field and decided whether to administer intravenous corticosteroid and whether or not to continue surgery. We regarded a 50% or greater decrease in amplitude from baseline of the D-wave or a 50% or greater decrease in amplitude or 10% or greater increase in latency of the SSEP to be significant.

TABLE 1. Wave Deterioration Rate and Postoperative Motor Deficits Rate in Each Disease Entity

Etiology	Cases	Wave Deterioration (%)	Postoperative Motor Deficits (%)
Scoliosis	19	6 (32)	0 (0)
Extramedullary spinal cord tumor	14	4 (29)	0 (0)
Intramedullary spinal cord tumor	10	7 (70)	5 (50)
OPLL	9	5 (56)	4 (44)
OYL	8	4 (50)	2 (25)
Disc herniation	4	0 (0)	0 (0)
Caries	4	1 (25)	0 (0)
Burst fracture	3	0 (0)	0 (0)
Spinal cord herniation	2	1 (50)	1 (50)
Metastatic tumor	2	0 (0)	0 (0)
Benign spinal tumor	1	0 (0)	0 (0)
	76	28 (37)	12 (16)

OPLL indicates ossification of the posterior longitudinal ligament; OYL, ossification of the yellow ligament.

Statistical Analysis

We compared the mean amplitude of baseline, minimum, and final TcMEP between muscles with or without postoperative motor deficits using Student t test, and we created receiver operating characteristic (ROC) curves to determine the cutoff amplitude. Sensitivity and specificity at optimal cutoff values were calculated with $P < 0.05$ considered statistically significant. Data analysis was performed with SPSS (Version 20 for Windows, IBM, Armonk, NY).

RESULTS

Descriptive

We obtained an acceptable and monitorable baseline TcMEP response from at least 1 muscle TcMEP in 76 surgeries. Twenty-eight patients (37%) experienced intraoperative electrophysiological deterioration defined as a 70% or greater decrease in TcMEP amplitude from baseline. In 12 of the 76 surgeries (16%), detectable postoperative muscle weakness was found at the most immediate postoperative examination. The etiology, wave deterioration rate, and postoperative motor deficit rate are shown in Table 1. Table 2 presents demographics and electrophysiological and neurological data of these 12 surgical procedures. There were 12 surgical procedures for 11 patients (6 males and 5 females). Number 1 and number 2 are 2 surgical procedures performed on the same patients. The average age at surgery was 46.4 years. Three patients sustained muscle weakness 6 months postoperatively; the others recovered fully. All these 12 surgical procedures with postoperative motor deficits demonstrated significant deterioration of TcMEP, and there were no false-negative cases. Other 16 cases which showed significant intraoperative deterioration of TcMEP but

TABLE 2. The Cases With Postoperative Motor Deficits

N	Age, yr	Sex	Etiology	Preoperative MMT	Intraoperative Wave Deterioration	Postoperative MMT	Postoperative 6 mo
1	40	F	T1–T3 ependymoma	5/5	All monitorable muscles	2/5 Lt. All muscles 4/5 Rt. All muscles	...
2	40	F	T1–T3 ependymoma	3/5 Lt. All muscles	All monitorable muscles	0/5 Rt. and Lt. All muscles	5/5 (more than 3 mo)
3	61	F	T1–T12 OPLL	4/5 Rt. Ilio, Quadriceps, ham	All monitorable muscles	0/5 Rt. and Lt. All muscles	2/5 Rt. and Lt. All muscles
4	42	M	T2–T12 OPLL	4/5 Rt. and Lt. Ilio, ham, TA	All monitorable muscles	1/5 Rt. and Lt. All muscles	5/5 (more than 3 mo)
5	64	M	T9–T11 OYL	4/5 Lt. All muscles	All monitorable muscles	3/5 Rt. and Lt. quadriceps	5/5 (within 1 W)
6	25	F	T12 hemangioblastoma	5/5	All monitorable muscles	3/5 Rt. and Lt. All muscles	5/5 (within 1 mo)
7	20	F	T3–T5 ependymoma	5/5	All monitorable muscles	3/5 Rt. and Lt. Quadriceps, AL, Ham	5/5 (within 3 mo)
8	59	M	T5–T6 spinal cord herniation	3/5 Rt. TA	Rt. TA	1/5 Rt. TA	2/5 Rt. TA
9	68	F	T6–T7 OYL	4/5 Rt. and Lt. Quadriceps, ham	All monitorable muscles	3/5 Rt. and Lt. Quadriceps, ham	5/5 (within 3 mo)
10	36	M	T5–T6 hemangioblastoma	4/5 Rt. All muscles	Lt. Quadriceps, ham Rt. Quadriceps, TA, Gc	3/5 Rt. Quadriceps	5/5 (within 1 mo)
11	63	M	T9/10 OPLL	4/5 Rt. and Lt. EHL, FHL	Rt. AL, TA, Gc Lt. Quadriceps, TA, Gc	1/5 Lt Gc, FHL	3/5 Lt Gc, FHL
12	39	M	T6–T12 OYL	4/5 Rt. and Lt. All muscles	Lt. Quadriceps, TA, AH Rt. AL, quadriceps, TA, Gc, AH	3/5 Rt. Quadriceps, TA	5/5 (within 1 mo)

Postoperative 6 mo status of no. 1 was not available because 3 months after the primary operation, secondary operation was performed (case No. 2).

MMT indicates manual muscle testing; F, female; M, male; Lt, left; Rt, right; OPLL, ossification of the posterior longitudinal ligament; Ilio, iliopsoars; Ham, hamstrings; TA, tibialis anterior; OYL, ossification of the yellow ligament; W, week; AL, adductor longus; Gc, gastrocnemius; EHL, extensor hallucis longus; FHL, flexor hallucis longus; AH, abductor hallucis.

TABLE 3. Successful Derivation Rate, Wave Deterioration Rate, and the Rate of Postoperative Motor Deficits Among 28 Cases With Significant Intraoperative Neurophysiological Deterioration.

Etiology	Objective Muscles	Monitorable Muscles (%)	Wave Deterioration (%)	Postoperative Motor Deficits (%)
Scoliosis	72	70 (97)	36 (51)	0 (0)
Extramedullary spinal cord tumor	48	38 (79)	19 (50)	0 (0)
Intramedullary spinal cord tumor	78	64 (82)	51 (80)	31 (48)
OPLL	60	43 (72)	43 (100)	29 (44)
OYL	48	41 (85)	31 (76)	12 (29)
Caries	12	12 (100)	9 (75)	0 (0)
Spinal cord herniation	12	2 (18)	1 (50)	1 (50)
Total	330	270 (82)	191 (71)	73 (27)

OPLL indicates ossification of the posterior longitudinal ligament; OYL, ossification of the yellow ligament.

no postoperative motor deficits were false-positive cases. The alarm criteria of 70% or greater decrease from baseline TcMEP amplitude results in substantially high false-positive rate.

Rate of Successful Derivation, Wave Deterioration, and Postoperative Motor Deficits

In the 28 patients who experienced significant intraoperative electrophysiological deterioration in at least 1 muscle, 330 muscles in the lower extremities had been chosen for monitoring. Of these 330 muscles, acceptable baseline TcMEP responses were obtained from 270 (82%) muscles. Of the 270 muscles with acceptable baseline responses, 191 (71%) had electrophysiological deterioration during the operation, and 73 (27%) muscles had postoperative muscle weakness (Table 3). This means that 73 muscles showed true-positive responses and 118 muscles showed false-positive responses when 70% criteria were applied.

TcMEP Amplitude

We compared the baseline TcMEP amplitude, the intraoperative amplitude decrease, and the final amplitude measurements from the 197 muscles without postoperative motor deficits and 73 muscles with postoperative motor deficits. The baseline amplitude did not differ significantly, but both the minimum intraoperative amplitude and the final amplitude were significantly greater ($P < 0.001$) in the muscles without postoperative motor deficits than those in the muscles with postoperative motor deficits (Figure 1).

ROC Analysis

We performed ROC analysis to identify the intraoperative and end-of-surgery TcMEP cutoff amplitudes that predict postoperative motor deficits. Figure 2 shows the ROC curve defining the cutoff amplitude at the deterioration point during surgery as an absolute value (μV) and a relative value (%) compared with the baseline amplitude. Figure 3 shows the ROC curve with both absolute and relative values defining the cutoff amplitude at the end of surgery. Table 4 shows the sensitivity and specificity for predicting postoperative motor deficits and the area under the receiver operating characteristics curve for each cutoff point.

Wave Recovery

The mean amplitude was significantly (2.5-fold) greater at the end of surgery in the group of muscles with postoperative motor deficits than that in the muscles without postoperative

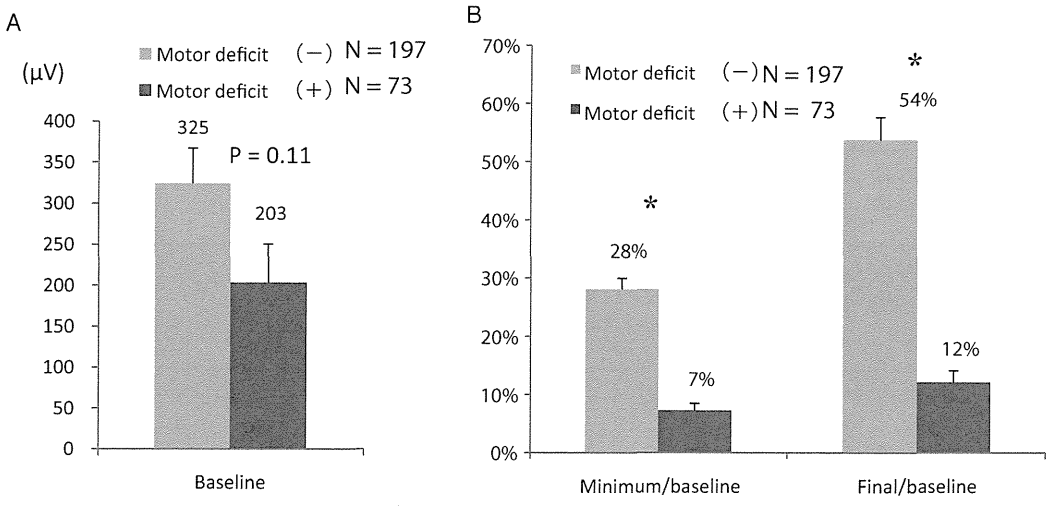

Figure 1. Mean amplitude of transcranial motor-evoked potentials at baseline in microvolts (**A**), at the deteriorated point, and at the end of the operation in percentage of control amplitude (**B**) among muscle groups with and without postoperative motor deficits. Results are shown as mean ± SEM (error bars). *$P < 0.001$.